Garwood, Gerri

From: Cathe Kalisz <kaliszc@api.org>
Sent: Monday, March 30, 2015 10:56 AM
To: Garwood, Gerri
Cc: Schaffner, Karen S.; Gary Mueller; Scott Evans (sevans@cleanair.com); vschmid@cleanair.com
Subject: Flare NOx Information et al.
Attachments: Copy of API Flare NOx Analysis v4 corrected EPA NOx NHV.xlsx; IFC_LiteratureReview.pdf; Copy of CRU-THC-MotivaPortArthur.xlsx

Gerri,

As requested during our March 25 meeting, attached are:

Flare NOx Data

- CAE spreadsheet with flare NOx data used for emission factor development
- Copy of IFC literature review report.
- The NOx calibration and QA/QC data were not published in a separate IFC report; we are working with IFC to see if the data can be provided.

Process Unit Test Data

- Attached is a summary of the Motiva Pt. Arthur process (feed rate) and test data for the ICR CRU test. It appears this test was inadvertently excluded in EPA's CRU emission factor review.

Please let us know if you have any questions,

Regards,

Cathe

Cathe Kalisz, P.E.
Policy Advisor
Regulatory and Scientific Affairs
American Petroleum Institute
1220 L Street NW
Washington, DC 20005
PH: (202) 682-8318
FAX: (202) 682-8270
kaliszc@api.org

Natural Resources Canada | Ressources naturelles Canada

CanmetENERGY

Leadership in ecoInnovation

Emissions from Elevated Flares – A Survey of the Literature

P. Gogolek, A.Caverly — CanmetENERGY- Ottawa

R. Schwartz — John Zink Company LLC

J. Seebold — Consultant

J. Pohl — Energy International

Prepared for the International Flaring Consortium

April 2010

Funding provided by members of the International Flaring Consortium

BP	ExxonMobil	Saudi Aramco
Chevron	John Zink Company LLC	Shell
DuPont	NOVA Chemicals	Total

Canada

DISCLAIMER

This report was prepared by CanmetENERGY as an account of work funded by the International Flaring Consortium (IFC). CanmetENERGY has made all reasonable efforts to ensure the exactness of the information provided in this report and the opinions expressed herein are those of CanmetENERGY solely. However, neither CanmetENERGY, the International Flaring Consortium, nor any person acting on behalf of them;

a. Makes any warranty or representation, expressed or implied with respect to the accuracy, completeness, or usefulness of the information contained in this report, or that the use of any information, apparatus, method, or process disclosed in this report may not infringe privately-owned rights, or

b. Assumes any liability with respect to the use of, or for damages resulting from the use of, any information, apparatus, method, or process disclosed in this report.

Reference to specific commercial products in this report does not represent or constitute an endorsement, recommendation, or favoring by CanmetENERGY, the International Flaring Consortium, nor any person acting on behalf of them, of the specific manufacturer or commercial product. The involvement by CanmetENERGY in this project is not to be used for promotional purposes beyond being identified as an independent third party evaluator.

TABLE OF CONTENTS

1.0 Introduction 1

2.0 Survey of Published Work 7

2.1 Analysis of Published Work 7

2.2 Published Work Conclusion 30

3.0 Analysis of Major Variables Affecting Performance 32

3.1 Fluid Mechanical Regimes 32

3.2 Flare Gas Composition 38

3.2.1 Jetting Regime 38

3.2.2 Buoyant Regime 40

3.2.3 Wake-stabilized Regime 41

3.3 Combustion Properties of Gas Mixtures 41

3.3.1 Mixing Rules 42

3.3.2 Mixing rule for flammability limits 43

3.3.3 Mixing rules for laminar flame speed 49

3.4 Flare Gas Rate 52

3.4.1 Jetting Regime 52

3.4.2 Wake-stabilized regime 53

3.5 Wind Speed 53

3.5.1 Jetting Regime 53

3.5.2 Wake-stabilized Regime 54

3.6 Steam Assist 55

3.7 Flare Diameter 56

3.7.1 Jetting Regime 57
3.7.2 Wake-stabilized regime 58
3.8 Scale-up and Dimensionless Parameters 58
3.8.1 Explaining the '3 inch Rule' in the Jetting Regime 59
3.8.2 Explaining the '3 inch Rule' in the Wake-Stabilized Regime 60
3.8.3 Dimensionless parameters 62
3.9 Conclusion on Major Variables 63
4.0 Trace Emissions 64
4.1 Hydrocarbon Emissions 65
4.2 NO_x Emissions 69
5.0 Conclusions 70
6.0 References 73
7.0 Appendix 80

LIST OF FIGURES

Figure 1 - The effect of steam rate on combustion efficiency for propylene flaring from the CMA study (McDaniel [1983]). 12

Figure 2 - The effect of nitrogen dilution of propylene on combustion efficiency without steam assist, from the CMA study (McDaniel [1983]). 14

Figure 3 - Lift-off data for hydrogen diluted with nitrogen from EER[1997] without a pilot burner, with the correlation for stability with and without a pilot burner. 19

Figure 4 - Fuel detection downwind of flare tip in wake-stabilized mode of operation as reported in Johnson et al. [2000]. 21

Figure 5 - Reproduction of Figure 6 in Howell et al. [2003]. 22

Figure 6 - The data from Figure 5 recalculated to give the combustion inefficiency (CI) and put ±100% bands on equation (2-6). Log-linear plot allows the data for the different pipe sizes to be easily distinguished. 23

Figure 7 - Comparison of the combustion inefficiency results for 2.5 cm (1") pipe firing natural gas from the large-scale University of Alberta tests with those from the CanmetENERGY FTF, plotted against the buoyant plume parameter (equation 2-5). 25

Figure 8 - Comparison of the combustion inefficiency results for 5.1 cm (2") pipe firing natural gas from the large-scale University of Alberta tests with those from the CanmetENERGY FTF, plotted against the buoyant plume parameter (equation 2-5). 26

Figure 9 - Comparison of the combustion inefficiency results for 10.2 cm (4") pipe firing natural gas from the large-scale University of Alberta tests with those from the CanmetENERGY FTF, plotted against the buoyant plume parameter (equation 2-5). 27

Figure 10 - Combustion Inefficiency for natural gas diluted with 60%-vol nitrogen and carbon dioxide, 10.2 cm (4") pipe. The flame blew out at the top wind speed of 43 km/h (27 mph) with carbon dioxide dilution. Data from Gogolek and Hayden [2004]. 28

Figure 11 - Schematic regime map of fluid mechanical behaviour for elevated flares. 34

Figure 12 - Plot of Strouhal number for a cylinder against cross-flow Reynolds number. 36

Figure 13 - Static drag coefficient and the dynamic force coefficient for a cylinder as a function of the crossflow Reynolds number. 37

Figure 14 - Flammability diagram for methane, after Zabetakis [1965]. 45

Figure 15 - Comparison of calculated lower flammability limit of methane/hydrogen/inert systems with measured lower flammability limit data from Karim, et al [2004]. Different values of nitrogen equivalence for carbon dioxide are used. 47

Figure 16 - Flammability diagram for methane with piece-wise linear representation given by the coloured lines. 48

Figure 178 - Plot of the ratio of viscous boundary layer thickness to pipe diameter (BL) against pipe diameter for flare gas exit velocities in the observed range of maximum stable velocity. 60

Figure 18 - Wind Reynolds number for pipe sizes from pilot-scale to full-scale. The various regimes for the wake of a long cylinder are indicated. 61

Figure 19 - Measured VOC emissions at the CanmetENERGY FTF as the mass of VOC in volume of stack gas. The compounds emitted from natural gas with gasoline can be attributed to unburned components in the gasoline. 67

Figure 20 - Concentration of PAH species in the soot emitted from flares from the CanmetENERGY FTF firing propane and the CMA tests firing raw propylene (McDaniel [1983]). The abbreviations are given in Table 7. 68

Figure 21 - The effect of nitrogen dilution of propylene on combustion efficiency without steam assist, from the CMA study (McDaniel [1983]). 80

Figure 22 - Lift-off data from EER[1997] without a pilot burner, with the correlation for stability with and without a pilot burner. 81

Figure 23 - Combustion Inefficiency for natural gas diluted with 60%-vol nitrogen and carbon dioxide, 4" pipe. The flame blew out at the top wind speed of 27 m/h with carbon dioxide dilution. Data from Gogolek and Hayden [2004]. 82

Figure 24 - Plot of the ratio of viscous boundary layer thickness to pipe diameter (BL) against pipe diameter for flare gas exit velocities in the observed range of maximum stable velocity. 82

Figure 25 - Wind Reynolds number for pipe sizes from pilot-scale to full-scale. The various regimes for the wake of a long cylinder are indicated. 83

Figure 26 - Measured VOC emissions at the CanmetENERGY FTF as the mass of VOC in volume of stack gas. The compounds emitted from natural gas with gasoline can be attributed to unburned components in the gasoline. 84

LIST OF TABLES

Table 1 - RRG compositions used by Seigel [1980] on a volume % basis. 9

Table 2 - RRG compositions used by Siegel [1980], including average, maximum and minimum contents on a volume % basis..... 9

Table 3 - Summary of the combustion efficiency data for the CMA trials (McDaniel [1983])..... 13

Table 4 - Combustion properties of selected combustible gases [Source: Baukal and Schwartz (2001)] and suggested range of steam-to-fuel ratio (SFR) from API Standard 521, Table 11. 40

Table 5 - Nitrogen equivalence values for carbon dioxide and water vapour reported in Molnarne et al. [2005], with values obtained by fit to flammability diagrams of Zabetakis [1965]. 46

Table 6 - Tabulation of piece-wise linear representation of flammability diagrams for selected fuels diluted with nitrogen and carbon dioxide..... 49

Table 7 - List of abbreviations of PAHs used in Fig. 20. 68

Table 8 - Combustion properties of selected combustible gases. 84

NOMENCLATURE

α_i	Coefficients for Spalding's flame speed mixing rule, equation 3-18.
Δ	Ratio of boundary layer thickness to pipe diameter
δ	Thickness of boundary layer at inside pipe wall, (m)
ε_x	Emission factor based on mass release rate, Equation 4-1
η	Combustion efficiency
$\overline{\eta}$	Average combustion efficiency
k_{CO_2}	Multiplier for laminar flame speed with CO_2 dilution
k_{N_2}	Multiplier for laminar flame speed with N_2 dilution
ν_a	Kinematic viscosity of air (m^2/s)
ν_f	Kinematic viscosity of fuel gas (m^2/s)
ρ_a	Density of air, (kg/m^3)
ρ_f	Density of fuel gas, (kg/m^3)
ρ_p	Density of burnt fuel products, (kg/m^3)
$\overset{\cap}{\rho}$	Density of gas for use for steam-assisted flare gas jet, Equation 3-30, (kg/m^3)
x_{CO_2}	Mole or volume fraction of CO_2 in gas mixture
$x_{H_2 lift-off}$	Mole fraction of H_2 at lift-off
x_i	Mole or volume fraction of species i in gas mixture
x_{N_2}	Mole or volume fraction of N_2 in gas mixture
AFR_L	Air-fuel volume ratio at lower limit
AFR_{ST}	Air-fuel volume ratio for stoichiometric mixture
AFR_U	Air-fuel volume ratio at upper limit
AL	Acenaphthylene (a PAH)
AN	Anthracene (a PAH)
A_p	Open area of flare pipe (m^2)
ARC	Alberta Research Council.

B(a)A	Benz(a)anthracene (a PAH)
B(ghi)F	Benzo(ghi)fluoranthene (a PAH)
BP	Buoyant Plume parameter, defined in equation 2-5 (dimensionless).
CCE	Carbon Conversion Efficiency, the mass percentage of carbon in the flare gas converted to carbon dioxide (%).
C_d	Drag coefficient
CE	Combustion Efficiency (%).
Chrysene	Chrysene (a PAH)
C_l	Dynamic force coefficient
CI	Combustion Inefficiency, = 100% - CE (%).
CMA	Chemical Manufacturers Association.
D^*	Dimensionless pipe diameter, Equation 3-32.
DE	Destruction Efficiency, the percentage of a species in the flare gas that is converted into any other species. DE = 100% - FS.
D_{eq}	Equivalent pipe diameter, Equation 3-30, (m)
D_p	Diameter of flare pipe (m)
EER	Energy and Environmental Research Corporation
E_x	Emission factor based on heat release rate, Equation 4-1
F_d	Dynamic Force on cylinder in cross-flow, (N)
FL	Fluorene (a PAH)
FL_i	Flammability limit of a compound, either upper or lower.
FL_{mix}	Flammability limit of mixture, either upper or lower.
FLT	Fluoranthene (a PAH)
Fr	Froude number, Equation 3-1
F_s	Steady Force on cylinder in cross-flow, (N)
FS	Fuel Slip (%) $FS = 100\% - DE$
FTF	Flare Test Facility
FTIR	Fourier Transform Infrared Spectrometry
f_v	Frequency of vortex shedding, s^{-1}.
g	Acceleration due to gravity (m/s^2)
G_{tot}	Total linear momentum,

H_f	Flame length, (m)
I*	Maximum inert concentration, see Figure 17
L*	The location where the Lower Flammability Level is reached, see Figure 17
LCCE	Local Carbon Conversion Efficiency, the CCE based on the measurements at a point.
LHV_m	Lower Heating Value, mass basis (MJ/kg).
LHV_v	Lower Heating Value, volume basis (MJ/m^3)
LFL	Lower Flammability Limit, (vol-%)
$\dot{m}_f$	Mass flow of fuel gas (kg/s)
Ne	Nitrogen-equivalence Factor
n_i	Number of moles of product from complete combustion of one mole of fuel at stoichiometric conditions
PAH	Polycyclic Aromatic Hydrocarbon
PF	Power Factor, defined in equation 2-7 (dimensionless).
PHE	Phenanthrene (a PAH)
PY	Pyrene (a PAH)
$\dot{Q}$	Heat release rate, (MW)
R	Momentum flux ratio of jet to cross-wind, Equation 3-1
Re	Reynolds number
Re_f	Reynolds number, flame-based, Equation 2-3
Re_p	Reynolds number for flow inside a pipe
Re_w	Reynolds number for pipe in cross-wind
Ri	Richardson number
RRG	Refinery Relief Gas, general term for the gases sent to the flares.
S	Laminar flame speed, (m/s)
SA_m	Stoichiometric air-to-fuel ratio, mass basis
SA_v	Stoichiometric air-to-fuel ratio, volume basis
SFR	Steam-to-Fuel Ratio, the mass ratio of steam-assist to flare gas (kg/kg).
S_{max}	Maximum laminar flame speed or burning rate, (m/s)
S_{st}	Laminar flame speed or burning rate at stoichiometric air, (m/s)
S_t	Strouhal number

T_{ad}	Adiabatic Flame Temperature, (K)
$\hat{T}_e$	Effective activation temperature in Equation 3-19, (K)
U^*	The location where the Upper Flammability Level is reached, see Figure 17
U_{bo}	Gas exit velocity at blow-off, Equation 2-1
U_f	Exit speed of fuel gas (m/s).
UFL	Upper Flammability Limit,(vol-%)
U_w	Mean crosswind speed, m/s, Equation 2-7
U_w^t	Modified wind speed in Equation 3-4, (m/s)
V_a	Acoustic velocity (speed of sound) in flare gas, Equation 3-25
V_f^*	Dimensionless exit velocity, Equation 3-32
w_i	Weight fraction of species i in gas mixture
w_x	Weight fraction of species x in gas mixture

1.0 INTRODUCTION

Flares are an essential safety technology for the clean and economical disposal of combustible gases. They have been operating in refineries, chemical plants, steel mills, and other industries for over fifty years. These decades have seen the incremental improvement of the technology – smoke suppression, robust pilots, scale-up, monitoring. There have also been periods of intense scientific research increasing our understanding of the factors affecting flare performance, and quantifying the emissions from flares. Even so, there remains a fair amount of work that needs to be done.

There are numerous difficulties in taking measurements from operating industrial flares. These include very high stacks (100 m or more), dangerous heat radiation to personnel and varying flame position due to changing flare gas flow rates and wind speed. The measurements on an operating flare give sparse coverage of the range of possible operating conditions and makes scientific conclusions difficult. This requires measurements to be taken on pilot-scale flares with controlled operating conditions or using remote sensing technology. The question of scale-up of pilot-scale measurements then becomes central. However, extractive techniques are either single- or multi-point probes, hood capture, or wind tunnel. Each has its own strengths and weaknesses.

Point Probes: A single probe is traversed across the diameter of the plume of combustion products. Generally the velocity profile is assumed to be Gaussian, as for an non-reacting free jet. The composition profile and velocity profile together give the flux of material, which is compared to the influx of combustible material to the flare stack. A rake of probes may also be used, giving a fixed sampling grid and more rapid coverage of the plume. A tracer gas may or may not be used.

Natural wind will make this technique difficult to use, since the plume will be pushed around unpredictably. A man-made wind, using a blower or a wind tunnel, would hold the plume trajectory steady and permit probing. However, the velocity profile would no longer be Gaussian (Rajaratnam 1976). A tracer gas could be used to ascertain the material flux.

Hood Sampling: In this technique, a hood and stack are placed over the flare tip, above the flame tip to capture the products of combustion. A fan is placed in the stack to provide suction to capture the combustion products. Samples are extracted from the stack. These samples are well-mixed and there is no need to assume a velocity profile for the plume and it is less vulnerable to plume displacement by wind. However, some of the plume can be lost and air is entrained by the suction applied to the hood. An inert tracer is required to estimate the dilution by air entrainment. The assumption is made that any combustion products lost have the same composition as those captured by the hood.

Wind Tunnel: The model flare is placed inside a wind tunnel. The wind is controlled and all the combustion products are kept within the wind tunnel. Point sampling can be used to map the concentrations. However, sampling probe located downstream of the flare, where a uniform velocity and composition profile has been established, means there is no need to estimate entrainment or assume a velocity profile. The walls of the wind tunnel must be cooled to avoid artificially stabilizing the flame with back-radiation. However, the fixed size of the wind tunnel constrains the size of the flare that can be tested. There has to be a wind present, otherwise the vertical rise of the flame will impinge on the ceiling of the wind tunnel. A recirculating wind tunnel will return combustion products to the reaction zone, making measurement of trace emissions problematic. A single-pass wind tunnel will bring in ambient air that can change during a run.

Remote Sensing: The extractive techniques are not applicable to operating flares, except for the smallest sizes and low firing rates, and on calm days. Remote measurement techniques are required to obtain measurements on full-scale flares at refineries or chemical plants. These involve some method of examining the radiation spectra of the flare plume. It can either be the emission spectrum from the hot combustion gases or the transmission spectrum when the source and receptor are on opposite sides of the plume. The source could be sun light. This technique gives line of sight measurement along a path through the plume. The concentration profile of the plume can be reconstructed in the manner used in tomography. This is potentially a very powerful technique, but it has several weaknesses. Fluctuations in the plume due to wind turbulence and gusting can interfere with the tomographic calculations, in the same way that moving during a

medical scan can ruin the results. A velocity profile has to be assumed or measured by an independent method, and with a variable wind the velocity determination may not coincide with the concentration measurements. The measurement is a line-average of the concentration along the full path, so interference by the ambient air can be a problem. Some techniques rely on the radiation of hot gases in the plume, the temperature of which needs to be known or estimated. Finally, the system may not be able to measure all species of interest, particularly trace organic compounds.

Note that there have been no successful blind-validation comparisons with reliable extractive-sampling tests of any remote sensing technology. Thus, while 'point-and-shoot' measurement technology is needed and desired by operators and regulators, it has yet to be proven to provide quantification of speciated mass emissions of today's highly-reactive volatile organic compounds of interest (e.g., ethylene, propylene, butadiene) or the class-archetypal carcinogens of interest (e.g., formaldehyde, benzene, benzo(a)pyrene). In short, there are at the moment of writing, and to the authors' best knowledge, no proven remote sensing techniques for speciated flare mass emissions.

This is a review of the published literature as it pertains to the emissions from elevated flares, assisted or not, for upstream or downstream application in the petroleum and chemical industries. We have attempted to be thorough. Mathematical models of flares, whether simple analytical treatments or large scale computer simulations, are not treated here. It is a topic deserving its own review.

The survey of the literature is followed by a detailed analysis of the results for the effects of important operating parameters, namely flare gas composition and exit velocity, flare tip size, cross-wind speed, assist medium and assist rate. We also highlight the data on the trace emissions. We end the review with a discussion of the scaling of flares, as applied to emissions, the "3 inch rule", and the dimensionless groups that may be useful in correlating the emissions from flares.

Dubnowski and Davis [1983] provided an excellent review of the state-of-the-art in the early stages of the intense activity in the 1980's. Twenty years later, the authors and other leading researchers briefly reviewed the most significant of the contributions to flare emissions research of the last three decades in Seebold et al. [2003]. This provided the

background perspective of researchers who were directly involved in leading and executing the 1980's flare efficiency studies that formed the foundation for future studies. This review is an elaboration of that paper with a detailed and critical examination of the published data. The intention is to identify the reliable knowledge, the apparent contradictions, the errors, and any gaps remaining.

Note on terminology: We use the following definitions of performance measures.

- **Carbon Conversion Efficiency (CCE)**:= the conversion of fuel-bound carbon to carbon dioxide, expressed as a percentage of the mass of carbon as carbon dioxide in the stack gas relative to mass of fuel-bound carbon.
- **Carbon Conversion Inefficiency (CCI)**:= the failure to convert fuel-bound carbon to carbon dioxide, CCI = 100% - CCE.
- **Fuel Slip (FS)**:= percentage of mass of carbon as original fuel species in stack gas relative to the mass of fuel-bound carbon.
- **Destruction Efficiency (DE)**:= the destruction of a particular combustible species, expressed as percentage of 100% minus the mass of carbon of the combustible species in the stack gas relative to the mass of fuel-bound carbon of that combustible species. For a single hydrocarbon species, DE = 100% - FS.

1.1 Overview of CFR40 Requirements

Landmark studies sponsored by the United States Environmental Protection Agency (EPA) in the early 1980s (Pohl et al. [1984], Pohl and Solberg [1985, 1986]) demonstrated that properly designed and operated industrial flares are highly efficient. These EPA-sponsored studies led EPA to the codification of the conditions that ensure the proper operation of industrial flares.

> "EPA determined the destruction efficiency of flares combusting volatile organic emissions in the early 1980s and developed the existing flare specifications as a result of this work."

The Control Device Requirements of 40CFR60.18 were issued by EPA as a final rule on January 21, 1986.

The requirements of 40CFR60.18 apply to control devices including flares that are used to comply with New Source Performance Standards (NSPS) promulgated by EPA under Section 111 of the Clean Air Act (CAA) and the National Emission Standards for Hazardous Air Pollutants (NESHAP) issued under the authority of Section 112 prior to the CAA Amendments of 1990.

The Control Device Requirements of 40CFR63.11 were issued by EPA as a final rule on March 16, 1994. The requirements of 40CFR63.11 apply to control devices including flares that are used to comply with NESHAP issued under the authority of the CAA Amendments of 1990 for the control of hazardous air pollutants (HAP).

Operating conditions for flares are specified at 40CFR60.18(b) through (d); and 40CFR 63.11(b).

> "Flares operating in accordance with these specifications destroy volatile organic compounds (VOC) or volatile hazardous air pollutants (HAP) with a destruction efficiency of 98 percent or greater."

The flare specifications originally contained in 40 CFR 60.18 and 40 CFR 63.11 were based upon experience with waste streams containing organic substances. The rules mandate that flares be designed for, and operated with, no visible emissions, except for periods not to exceed a total of five minutes during any two consecutive hours. In addition, the flare specifications require that the flare must be operated with a flame present at all times. The presence of a flare pilot flame is to be monitored to ensure that a flame is present at all times. The minimum net heating value of the flared gas and the maximum exit velocity of steam-assisted, air-assisted, and non-assisted flares are specified in a table.

The table lists the allowable velocities for the possible heat contents and an equation is provided to calculate the net heating value of the flared gas. Air-assisted flares must operate with an exit velocity less than a specified maximum allowable velocity which is calculated from an equation that is provided. Also, an equation is provided to calculate the maximum exit velocity for non-assisted and steam-assisted flares.

Additionally, at 40CFR60.18(c)(3)(ii), EPA specified the minimum net heating value (Btu/scf) of the flared gas to assure flame stability and high destruction efficiency. However, E.I. DuPont de Nemours and Company (DuPont), among others, recognized that the net heating value (Btu/scf) of the flared gas hardly told the whole flame stability story.

In particular, DuPont and others recognized that the requirement to enrich the flared gas by injecting a higher-energy gas such as natural gas should be unnecessary when flaring a gaseous mixture that, merely by virtue of the presence of hydrogen, has a heating value that is less than that required by 40CFR60.18(c)(3)(ii).

DuPont (EER [1997]) carried out a comprehensive testing program that led EPA to conclude that

> "... hydrogen-fueled flares achieve greater than 98 percent destruction efficiency."

Subsequently, in the only substantive change in the operating condition requirements to this day, EPA amended the 40CFR60.18 and 40CFR63.11 specifications to allow compliance by adhering either to the heat content specifications that had already been set out for organic-mixture flares; or, in the case of hydrogen-mixture flares having a hydrogen content of 8.0 percent (by volume) or greater, by utilizing flares with a diameter of 3 inches or greater that are designed for and operated with an exit velocity less than 37.2 m/s.

Today's provisions can be found at the following links:

40CFR60.18: http://edocket.access.gpo.gov/cfr_2009/julqtr/pdf/40cfr60.18.pdf
40CFR63.11: http://edocket.access.gpo.gov/cfr_2009/julqtr/pdf/40cfr63.11.pdf

2.0 SURVEY OF PUBLISHED WORK

There has been some impressive work on the performance and emissions from elevated flares and it is surveyed here. What is not covered is the work done on the properties of the flare flames, such as length, spread, and trajectory in a cross-wind, unless these are directly related to the combustion performance. Also not included are mathematical models and computer simulations. While there is some reason to believe that the predictions of the most sophisticated current computer simulations are close to the observed behaviors, it is beyond the scope of this survey.

The performance of flares is generally given by the combustion efficiency and destruction efficiency. The carbon conversion efficiency is defined as

$$CCE = 100\% \times \frac{net\ mass\ rate\ of\ C\ as\ CO_2\ in\ products}{mass\ rate\ of\ combustible\ C\ in\ flare\ gas} \tag{2-1}$$

For the combustion of hydrocarbons this is also called the Combustion Efficiency, CE or η. For a non-hydrocarbon fuel like hydrogen sulphide (H_2S), an equivalent conversion can be defined for sulphur. The combustion inefficiency is $1-\eta$ or $CI = 100\% - CE$. The Destruction Efficiency is the destruction of a particular species in the flare gas in the flare flame.

$$DE_X = 100\% \times \left(1 - \frac{mass\ rate\ of\ species\ X\ in\ products}{mass\ rate\ of\ species\ X\ in\ flare\ gas}\right) \tag{2-2}$$

A related term is the fuel slip of species X, $FS_X = 100\% - DE_X$. These calculations can also be defined in terms of the measured concentrations of products, which is completely equivalent in most cases. It is simple to show that the destruction efficiency is never less than the combustion (carbon conversion) efficiency (DE ≥ CCE).

2.1 Analysis of Published Work

Research into the combustion performance of flares started in earnest in the 1970s. Becker [1974] published a limited number of results of flaring natural gas in a wind tunnel. The flare pipe was 20 mm in diameter, exit velocity was 20 m/s and cross-wind speed was 5 m/s and 10 m/s. The combustion efficiency was from 99.8% to 99.9%.

Straitz [1977, 1978] attempted to determine the combustion efficiency of a range of flares firing natural gas and propane. Flare tip diameters were 5.1 cm, 7.6 cm, and 15.2 cm (2", 3", and 6"). Steam assist was used. Wind interfered with the gas sampling and there were deficiencies in the instrumentation. He found low combustion efficiency (approximately 75%) during smoking conditions but better than 99% combustion efficiency with steam-assist to eliminate smoking. Excessive steam produced a decline in combustion efficiency. The very low combustion efficiency reported during smoking tests has been contradicted by subsequent studies.

In 1980, Siegel published his doctoral thesis (Siegel [1980]). This summarizes his experimental work on a pilot-scale flare firing a slip stream of refinery relief gas (RRG). This flare was steam-assisted, with a blower simulating the cross-wind. The flare tip was of commercial design, allowing 10 t/h (22000 lb/h), with a 70 cm (27.6") diameter at the tip. It had six steam injection nozzles. The gas flow ranged from 0.13 to 2.9 t/h (286 to 6600 lb/h). The steam-to-fuel ratio (SFR) ranged from 0 to 1.73 kg/kg. Simulated wind speed was up to 6 m/s (13.4 mph). RRG compositions are given in Tables 1 and 2. These had high hydrogen content and low inert gas content.

The combustion gases were sampled with a point probe that could traverse a grid above the flare flame or downwind of the flare flame when the blower was on. The local carbon conversion efficiency (LCCE) was calculated for the sampling points. The LCCE was always greater than 98% and was less than 99% in only four instances. Three of those were only marginally below 99% while the fourth was attributed to over-steaming (SFR = 1.75). Smoking flare flames had LCCE greater than 99%. Siegel did not find any correlation between combustion efficiency and the operating variables of flare gas flow rate and composition, steam rate and cross-wind speed.

Table 1 - RRG compositions used by Seigel [1980] on a volume % basis.

	1	2	3	4	5	6	7	8	9
H_2	69.36	17.8	43.7	56.1	63.3	63.1	55.7	50.4	50.6
H_2S	1.3	0.4	1.6	1.5	0	0	0	0	0.2
CH_4	8.9	8.9	10.5	11.6	12.3	10.6	11.9	12.6	13.8
C_2H_6	7.2	5.8	7.7	9	10.2	6	5.8	6.8	6.8
C_2H_4	0.04	0.06	0.05	0.02	0.01	0.01	0.02	0.02	0.01
C_2H_2	0	0	0	0	0	0	0	0	0
C_3H_8	5.5	21	18.4	12.8	6.9	4.6	4.5	18.3	11.8
C_3H_6	0.06	0.06	0.3	0.1	0.04	0.1	0.2	0.2	0.04
C_4	2.43	39.01	3.5	4.76	3.2	7.7	1.4	1.4	7.2
C_5	3.1	3.7	8.98	4	3.8	8	19.4	10.2	8.7
C_6	0	1.3	7.3	0	0	0	1.2	0.3	0
N_2	2.2	1.8	0	0	0	0	0	0	0.6
H_2O	0	0	0	0	0	0	0	0	0
CO_2	0	0	0	0	0	0	0	0	0

Table 2 - RRG compositions used by Siegel [1980], including average, maximum and minimum contents on a volume % basis.

	10	11	12	13	14	15	Average	Max	Min
H_2	45.4	63	63.4	53.4	58.8	64.1	54.5	69.36	17.8
H_2S	0	0	0	0.1	0	0.2	0.4	1.6	0
CH_4	10.3	13.9	12.3	11.5	6.7	7.4	10.9	13.9	6.7
C_2H_6	4.8	6.5	4.8	7.3	5	5.3	6.6	10.2	4.8
C_2H_4	0	0.02	0	0	0	0	0.0	0.06	0
C_2H_2	0	0	0	0	0	0	0.0	0	0
C_3H_8	4.2	3.5	7.6	6	4.3	4.2	8.9	21	3.5
C_3H_6	0	0.1	0.01	0	0	0	0.1	0.3	0
C_4	16.2	3	6	13.2	9.9	4.5	8.2	39.01	1.4
C_5	10.1	10.2	5.6	8.8	2.7	3.3	7.4	19.4	2.7
C_6	0	0	0	0	0	0	0.7	7.3	0
N_2	7.5	0	0	0	11.4	11.2	2.3	11.4	0
H_2O	1.7	0	0	0	1.8	0	0.2	1.8	0
CO_2	0	0	0	0	0	0	0.0	0	0

Lee and Whipple [1981] performed tests with a 5.1 cm (2") diameter perforated tip (35% open area). There was no assist gas used. Propane was the flare gas while helium was used as the tracer gas. Grab samples indicated destruction efficiency of propane greater than 99%. Continuous sampling found periodic releases of CO from the side of the flame, attributed to eddy stripping and quenching the combustion products. These eddies may have been produced by the perforated tip, which is considered to be an unusual flare tip design characteristic.

Blow-out stability of jetting flames, essentially model flares, was investigated by Kalghatgi in still air [1981a] and with an imposed crosswind [1981b]. He burned methane, propane, ethylene, acetylene, hydrogen and commercial butanes. Methane and propane were also diluted with carbon dioxide and air. The pipe size ranged from 1 mm to 12 mm. The pipe size was changed to accommodate the combustion chamber. The blow-out velocity was made dimensionless by the maximum burning velocity in air and correlated with the density ratio of fuel and air and a Reynolds number based on the flame length and maximum burning velocity.

$$\frac{U_{bo}}{S_{\max}}\left(\frac{\rho_f}{\rho_a}\right)^{3/2} = 0.017\,\mathrm{Re}_f\left(1-3.5\times10^{-6}\,\mathrm{Re}_f\right), \mathrm{Re}_f = \frac{S_{\max}H_f}{\nu_f} \qquad (2\text{-}3)$$

The inclusion of a crosswind produced a new behaviour. Pipe size was increased to 20 mm in some cases. There was blow-off at high fuel flow rates but also blow-out at low fuel flow rates. For a particular fuel, the stability curve showed a correlation between the fuel velocity and the wind velocity. The curves scaled by the pipe diameter. For moderate wind speed, the blow-off velocity increased from the value in still air. If the flame managed to attach to the pipe, it was stabilized and blow-out did not happen. The results for all fuels were correlated graphically with wind and fuel velocities normalized by the maximum flame speed, the flame Reynolds number, Re_f and the density ratio raised to the 3/2 power.

The Chemical Manufacturers Association (CMA) published the final report on their flare efficiency study in 1983 (McDaniel [1983]). These tests used a single probe located above the flare flame with SO_2 as the tracer gas. At that time it was expected that any products of incomplete combustion were emitted at the flare tip, justifying the single sampling point. Inefficiency or fuel loss around the perimeter would not have been captured in these tests. Raw propylene and propylene/nitrogen mixtures (heating value from 3 MJ/m^3 to 81 MJ/m^3 (80 Btu/scf to 2183 Btu/scf) were flared. Steam- and air-assist flare tips were tested. The SFR ranged from 0 to 123 kg/kg.

The steam-assist flare tip was the John Zink STF-S-8 with two pilot burners. The maximum rated capacity was 24,000 kg/h (53,000 lb/h) for crude propylene. The maximum propylene flow for these tests was 1426 kg/h (3,138 lb/h), 6% of full capacity. The exit velocity of the flare gas ranged from 0.66 m/s (2.17 ft/s) to 19 m/s (62.5 ft/s). The pilot burners gave total heat input of 583 MJ/h (552,600 Btu/h), less than 1% of the total heat input at the top propylene flow.

The inferred combustion efficiencies were better than 98% except when over-steaming, or with high exit velocity of low heat content gas. Table 3 gives the combustion efficiency data. Figure 1 shows the effect of steam addition with undiluted propylene. High combustion efficiency was obtained with SFR below 3.5 kg/kg, but decreased rapidly with higher SFR. However, there were two tests (numbers 52 and 53) with much higher SFR (77.5 and 123) that obtained relatively high combustion efficiency (95.8 and 99.4). These tests had very low flare gas flow and low steam flow.

Flaring high volumes of low heating value gases may also result in lower combustion efficiencies. Additionally, smoking flares do not necessarily indicate inefficient combustion. Figure 2 shows the effect of nitrogen dilution. A summary of the findings were published in Keller and Noble [1983] and R.R. Romano [1983].

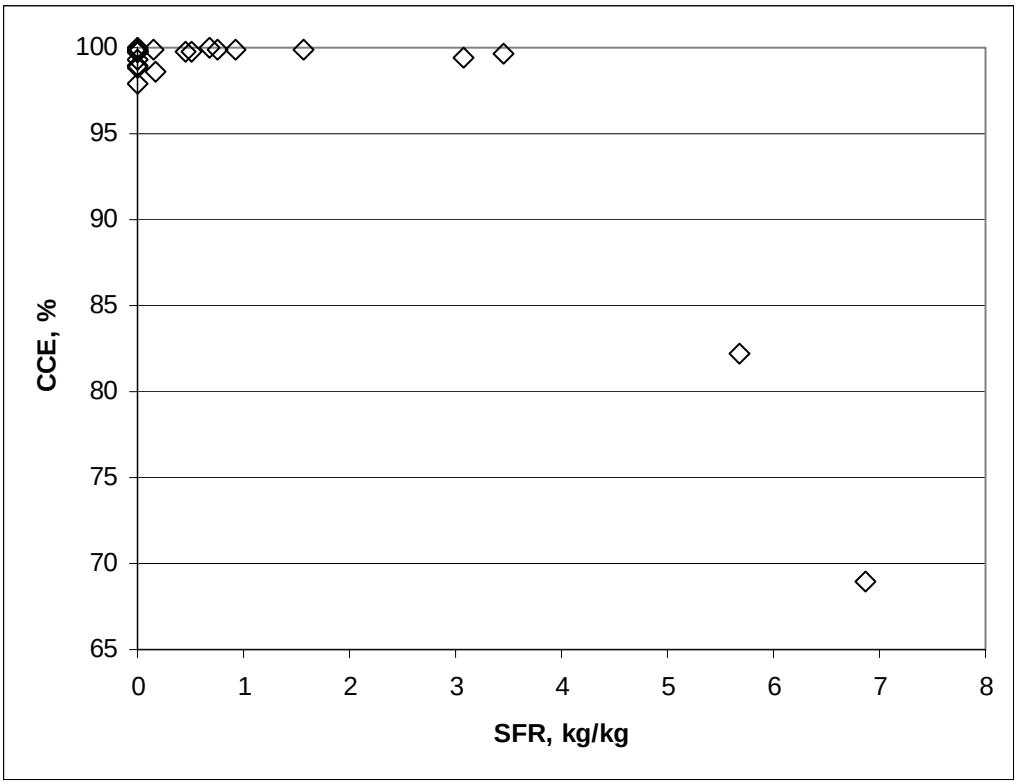

Figure 1 - The effect of steam rate on combustion efficiency for propylene flaring from the CMA study (McDaniel [1983]).

Table 3 - Summary of the combustion efficiency data for the CMA trials (McDaniel [1983]).

Run #	Gas Flow		Heat content		Nitrogen	SFR	CE
	Nm^3/min	Scfm	MJ/m^3	Btu/scf	vol%	kg/kg	%
2	788.3	464	81.72	2183	0.0	0.508	99.82
3	774.7	456	81.72	2183	0.0	0.448	99.82
1	803.6	473	81.72	2183	0.0	0.688	99.96
5	253.2	149	81.72	2183	0.0	1.56	99.94
	251.5	148	81.72	2183	0.0	0.725	
7	261.6	154	81.72	2183	0.0	0.757	99.84
17	41.6	24.5	81.72	2183	0.0	0.926	99.84
50	41.5	24.4	81.72	2183	0.0	3.07	99.45
51	552.2	325	11.57	309	85.8	0.168	98.66
23	0.839	0.494	9.99	267	87.8	0	100.01
52	0.945	0.556	10.0	268	87.7	77.5	98.82
53	0.605	0.356	7.82	209	90.4	123	99.4
54	0.605	0.356	7.82	209	90.4	0	99.9
4	480.8	283	81.72	2183	0.0	0	99.8
8	266.7	157	81.72	2183	0.0	0	98.81
55	42.0	24.7	81.72	2183	0.0	6.86	68.95
56	41.6	24.5	81.72	2183	0.0	3.45	99.7
11a	1121.3	660	11.4	305	86.0	0	99.79
11b	1017.7	599	12.8	342	84.3	0	99.86
11c	944.6	556	13.6	364	83.3	0	99.82
57	1194.4	703	11.0	294	86.5	0.15	99.9
16a	543.7	320	12.7	339	84.5	0	99.73
16b	428.1	252	15.3	408	81.3	0	99.75
16c	329.6	194	19.4	519	76.2	0	99.74
16d	270.1	159	23.7	634	71.0	0	99.78
59a	1004.1	591	7.19	192	91.2	0	97.95
59b	842.7	496	8.68	232	89.4	0	99.33
60	567.5	334	11.2	298	86.3	0	98.92
61		25		2183	0.0	5.67	82.18
	42.5		81.72				

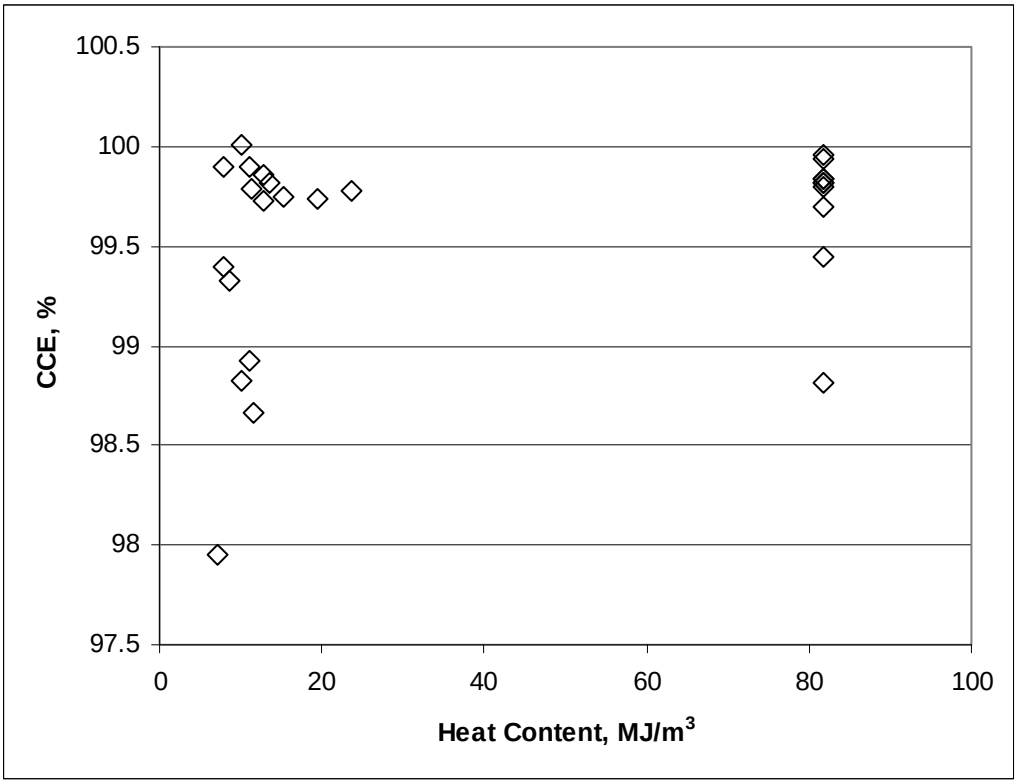

Figure 2 - The effect of nitrogen dilution of propylene on combustion efficiency without steam assist, from the CMA study (McDaniel [1983]).

The review of Dubnowski and Davis [1983] includes the CMA report and the early results from the Energy and Environmental Research Corporation (EER) work. They discuss the mechanisms of smoke suppression by steam injection, visible flame instability as an indication of reduced combustion efficiency, and the stability relationship between heat content of the flare gas and the exit velocity. They concluded that pilot-scale flares under controlled conditions were the best way to investigate the effect of operating parameters on performance. However, they also indicated that the appropriate scale-up procedure would be difficult to determine and eventually measurements on full-scale flares would be needed. This question of scale-up of pilot-scale results remains a hot issue. We will discuss this further in section 3.8.

Noble et al. [1984] investigated the stability of small flare flames with different gas compositions. They used a 7.6 cm (3") pipe to determine the maximum stable exit

velocity of natural gas, commercial propane and hydrogen diluted with nitrogen or carbon dioxide. After an excellent discussion of the combustion properties of mixtures, they presented an experimental index and correlated the maximum stable exit Mach number with this index (equation 3-25 below). They indicated that heat content of the flare gas is not adequate to predict flare stability.

The years from 1984 through 1986 saw published three reports on the work performed at EER for the US EPA on flare efficiency (Pohl et al. [1984], Pohl and Solberg [1985, 1986]). These landmark reports set the basis for existing regulation in the U.S. and appeared to have closed the book on research into flare performance.

Pohl et al. [1984] reported tests flaring propane and nitrogen mixtures, with 7.6cm, 15.2cm, 30.5cm (3", 6" and 12") diameter simple pipes, and three 30.5cm (12") diameter commercial flare tips. Both the rake and hood measurement techniques were used. Steam-assist was used in some of the tests. Wind was deliberated excluded from the testing. Two important correlations were produced:

1. Stability curve relating heat content to exit velocity at blow-out.
2. Combustion efficiency as a function of the heat content relative to the minimum heat content for stability.

They used the following determination of stability: flames near the stability limit are very sensitive to perturbations, and, when perturbed, can produce high emissions of unburned material. The stability curves showed that pipes less than 6.4cm (2.5") were not similar to larger pipes, that a 3" pipe gives similar stability behaviour to the 15.2cm and 30.5 cm (6" and 12") pipes, and that the simple pipe had similar stability behaviour to the 30.5 cm (12") commercial tips tested.

Combustion efficiency was better than 98% when the heat content of the propane/nitrogen mixture was above 1.1 times the minimum heat content determined from the stability curve. Near the stability limit the combustion efficiency can degrade significantly, and seems to be almost random. This degraded efficiency is the result of the sensitivity of the flame to perturbations. Out of 67 tests, measured flare efficiencies were >98% except for the two tests where the SFR exceeded 3.5. Also 98-99% flare

efficiencies were achieved for reduced flare gas rates when SFR was about 100. However, the effect of the pilot burners were likely dominating the flare gas combustion.

Pohl and Soelberg [1985] continued the work to look at flare design and gas composition. They selected several compounds that are particularly difficult to combust or have a strong propensity to smoke. They used the hood sampling technique for small flames and a tracer (SO_2) for large flames, to control the material balance. They found that the two correlations developed in the first report can be applied to different gas mixtures and different flare tip designs. They also found that flare tip design affects the stability curve. They concluded that the stability curve for a given flare tip and gas compound correlates the destruction efficiency in the same way as found in their first report. While Pohl et al. [1984] showed that 7.6 cm (3") pipes produce similar flames to larger pipes, they concluded that pipes less than 6.3 cm (2.5") diameter are not similar to the larger sizes. This places an important lower limit on pipe size that can be used for flare studies. This report includes results from the Flare Screening Facility where a very small pipe (either 0.2 cm or 0.3 cm (1/16 inch or 1/8 inch)) was used. They used this equipment for preliminary testing to expedite the pilot-scale work. They found that the maximum stable exit velocity and even the relative ranking of the gases did not correspond to the larger scale results. Pohl and Soelberg [1985] also reported on NO_x emissions. For hydrocarbon flare gas, the emission factor for NO_x was less than 0.04 g NO_2/MJ (0.1 lb NO_2/MMBtu). The emission factor for NO_x decreased with decreased heat release.

The third report in the series, Pohl and Soelberg [1986] treated H_2S and the effect of pilots. The tests used 7.6 cm and 15.2 cm (3" and 6") simple pipe flares. They found that H_2S/N_2 mixtures can be stably flared at significantly lower heat content than propane/N_2 mixtures. Destruction efficiency of H_2S and combustion efficiency of propane were better than 98% with heat content greater than 1.1 times the minimum stable limit, for both H_2S/N_2 and H_2S/propane/N_2 mixtures. This limit is closer to the minimum heat content than the limit found for propane/N_2 mixtures. When both H_2S and propane were in the mixture, the DE for H_2S was greater than the CE of propane. The two mixtures tested had 5% H_2S or 70% H_2S. Since H_2S is more reactive than propane, these results indicate that the more reactive species can be preferentially destroyed. They also indicate

that the presence of the highly reactive H_2S promotes the reactivity and the combustion of propane.

Flare efficiency depends on flame stability, which in turn depends on flare head design and flare gas exit velocity, heating value, and composition. There are practically as many different combinations of these variables as there are industrial flares. Therefore further research is needed on flare flames to improve and extend scaling factors, and to develop methods correlating the influences of gas mixture, flare head type, and operating conditions on the combustion and destruction efficiency for commercial flares.

This work, detailed in the three reports, set the operating envelope in U.S. EPA regulations for ensuring better than 98% combustion efficiency. It was a decade before the publication of significant new research on the combustion performance of flares.

Strosher[1996] reported results for tests on solution gas flares. The Alberta Research Council (ARC) tested solution gas flares typically found at oilfield battery sites in Alberta. In laboratory and pilot-scale tests, pure gas streams such as methane, propane and commercial natural gas were burned at high efficiency (98% or greater) under conditions typical of good operating practice. Co-flowing liquid hydrocarbon fuels or condensates in the pure gas streams degraded combustion efficiencies and crosswinds further reduced the combustion efficiency of co-flowing natural gas / condensate in the laboratory and pilot scale tests. At full scale, two oil field battery flares were tested. Both flares were rudimentary designs with no combustion enhancements such as knockout drums, flame retention devices or pilots and both flares experienced extensive liquid hydrocarbon carry-over. Accordingly, compared with properly designed and operated industrial flares, the combustion efficiencies of these field flares were expectedly degraded. The sweet-gas flare had more liquid carryover burned with combustion efficiency 62-71%. The second flare had sour gas and less liquid carry-over; it burned with combustion efficiency 82-84%.

These data were used in Leahey et al. [2001] to validate a simple mathematical model for the combustion efficiency of a flare flame. This model is based on the heat balance on the flame, using previously developed expressions for flame volume and surface area (Leahey and Schroeder [1987]). The model ignores the effect of liquid carry-over.

Regardless of the merits of the heat balance approach, Leahey et al. [2001] use a flame temperature of 1200ºC (2192ºF) in their calculations while the flame volume and surface area expressions were developed using a temperature of 1500ºC (2732ºF). This makes a substantial difference to the heat balance. Repeating the calculations with the correct flame temperature gives combustion efficiencies greater than 100%. It is clear that the model is much too simplistic to give realistic results with correct input data.

Boden et al. [1996] published remote sensing measurements on three operating flares using the DIAL (Differential Absorption LIDAR) technique. All three flares had steam-assist. Two were 106cm diameter and the third 122cm diameter (42" and 48" diameter). The DIAL measurements were set up for methane and the C2 to C6 alkanes. It did not measure other species that may have been in the plume, such as CO and olefins. The flare gases had high hydrogen content (50% to 78%) in three of the cases, 10% hydrogen in the fourth. The SFR was varied during the tests. The emissions of methane increased with increased SFR, but were less than 0.4% of the carbon in the flare gas. The emissions of higher alkanes decreased with increased SFR. They inferred from their results that the total combustion efficiency was better than 98% in all cases.

The DuPont study (EER [1997]) was concerned with the stability and destruction efficiency of low heat content flares with significant hydrogen content. They used a 7.4 cm (2.9") flare tip and the hood technique to collect and sample the combustion products. The study proceeded in two parts. The first was to determine the stability of the hydrogen flares. This was done through visual observation of the flame lift-off and blow-out, with and without a pilot burner. The results were correlated with a simple linear relation between exit velocity and hydrogen content (%v)

$$x_{H_2,lift-off} = 0.256U_f + 6.0 \qquad (2\text{-}4)$$

for fuel exit velocity from 5.0 m/s to 37.2 m/s (16.3 ft/s to 122 ft/s), with or without pilot burner. The hydrogen content ranged from 6%v to 15%v, as shown in Fig. 3; the balance was nitrogen. The heat content ranged from 0.6 MJ/m^3 to 1.5 MJ/m^3 (15 Btu/scf to 42 Btu/scf).

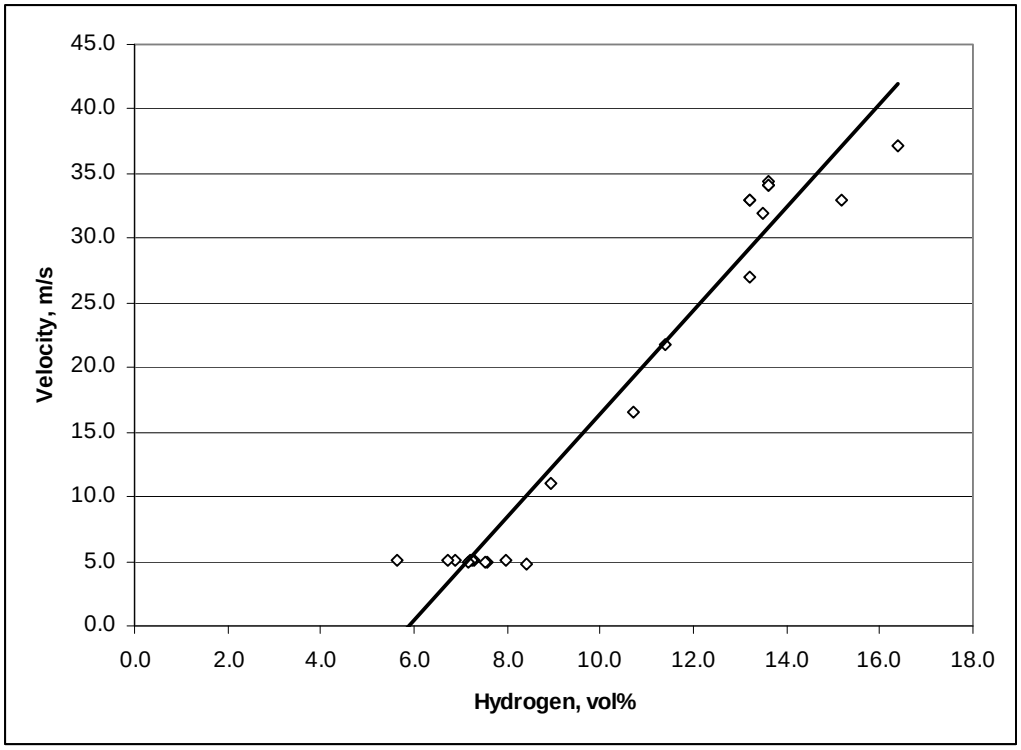

Figure 3 - Lift-off data for hydrogen diluted with nitrogen from EER[1997] without a pilot burner, with the correlation for stability with and without a pilot burner.

The second part of the study spiked the H_2/N_2 mixture with ethylene and measured the destruction efficiency of ethylene. As was found with the studies in the mid-1980s, destruction efficiency was better than 98% when the hydrogen content was at or above that for lift-off given by equation (2-4). Largely on the basis of these results, the regulations governing flares (40 CFR §60.18 and §63.11) were amended to include specific provisions for flaring of hydrogen-containing waste gases (U.S. EPA, Federal Register, May 4, 1998).

The following year started a series of publications from the University of Alberta concerning the efficiency of solution gas flares in Western Canada, and particularly the effect of wind. A particular characteristic of these flares is low momentum of the flare gas, with exit velocity of the solution gas less than the average wind speed of 4m/s to 7 m/s. They developed an experimental methodology using a closed-loop wind tunnel (Bourguignon et al. [1999]). Simple pipe flares with diameter 0.6 cm, 1.3 cm, and 2.5 cm (0.25", 0.5" and 1") were used in this facility. The maximum cross-wind speed was 14

m/s (31 mph). Commercial natural gas and propane were fired, as was ethane. Tests were done with carbon dioxide as an inert diluent. The subsequent series of papers chronicle the progress of the work on this facility at the University of Alberta. The main results are contained in the reports Kostiuk et al. [2000a,b] [2004]. It is important to remember that these tests were aimed at solution gas flares, which are very different from the large industrial flares. These differences include: simple tip design and small diameter, no steam or air assist, relatively simple flare gas composition, and CO_2 content. The results for these small and simple flares likely do not apply to the larger, more complicated industrial flares.

Johnson et al. [1998,1999a,b, 2000], and Johnson and Kostiuk [1999, 2000] showed that cross-wind speed has a strong negative effect on combustion efficiency and identified a different mode of combustion properly termed "wake stabilized". Here the flame is imbedded in the wake of the flare tip, protected from the cross-wind. This is quite different from the strong vertical flame studied previously. These papers also show the combustion inefficiency relationship between wind speed and flare gas exit velocity to be $U_w / U_f^{1/3}$. This factor collapsed the inefficiency data for different flaring rates onto a single curve. They continued to develop the dimensionless parameter based on a buoyant plume model of the flare flame,

$$BP = \frac{U_w}{\left(gD_p U_f\right)^{1/3}}. \tag{2-5}$$

However, there is uncertainty whether better fit to the experimental data is obtained with a square-root dependence on pipe diameter (Howell [2003]).

Johnson et al. [2000] used point-sampling in the downstream wake along the plane of the flare pipe in the neighbourhood of the flare flame to investigate the mechanism for inefficiency. The gas sample was sent to an on-line FID to detect the presence or absence of hydrocarbons. The wind speed was 8 m/s (26.2 ft/s) and the fuel exit velocity was 1 m/s (3.3 ft/s). The flare tip was a simple pipe with outer diameter of 2.47 cm (1") and inner diameter of 2.21 cm (0.9"). Figure 4 shows the map of the results. Fuel was detected in a narrow band along the top of the flame. Fuel was primarily detected below the flame in the flare wake, which is a region of low pressure. They proposed a fuel-

stripping mechanism of fluid flow in the near-wake pulling fuel out of the flame region to be quenched without undergoing significant reaction. Clearly the flow structure in the near wake of the flare pipe is the most important factor for the inefficiency of the flare flame with strong wind.

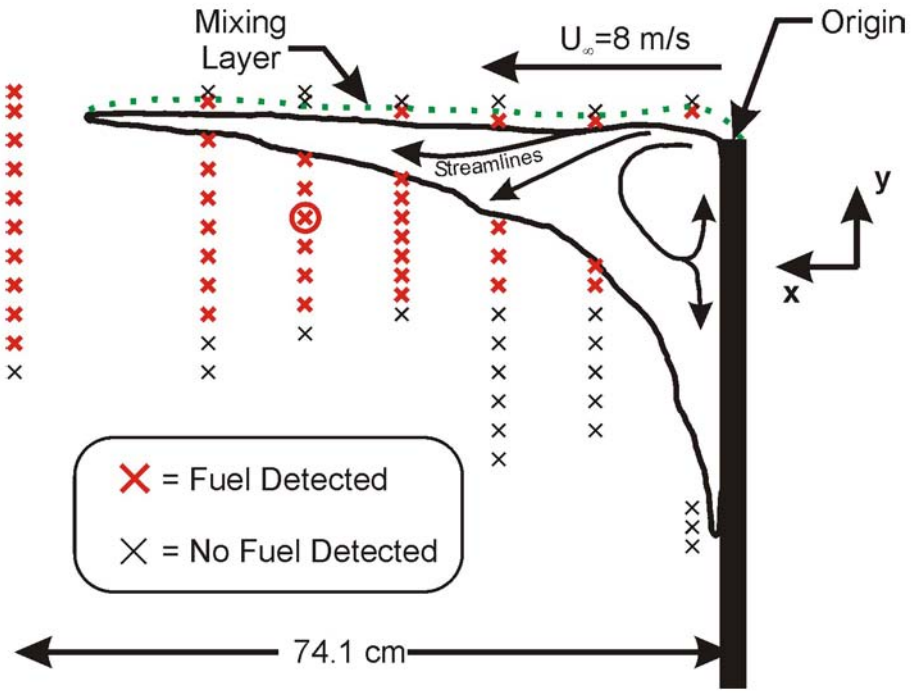

Figure 4 - Fuel detection downwind of flare tip in wake-stabilized mode of operation as reported in Johnson et al. [2000].

Johnson and Kostiuk [1999] report the comparison between natural gas and propane diluted with carbon dioxide. They found that carbon dioxide dilution weakens the flame and it could easily be blown out. The lower limit for heat content was around 10 MJ/m^3. They also diluted propane with carbon dioxide to the same heat content (lower heating value, volume basis) as natural gas, but the combustion efficiency of the propane/CO_2 mixture was greater than that of natural gas. They ultimately settled on the lower heating value on a mass basis as an adequate measure of the fuel composition effect. However, they had to treat "methane-like" and "propane-like" fuels separately.

The correlation they derived for combustion inefficiency was

$$\mathrm{CI}\left(\mathrm{LHV_m}\right)^3 = a\exp(bBP) \qquad (2\text{-}6)$$

where *a* and *b* are fit parameters, different for "methane-like" or "propane-like" gas. No rule was given for deciding which to apply, although ethane was considered "propane-like".

The work concluded with experiments in a much larger single-pass wind-tunnel with larger pipes. The pipes tested were 2.5 cm, 5.1 cm, and 10.2 cm (1", 2" and 4") diameter. A rake system was used to sample the combustion gases. These experiments were intended to verify the scale-up validity of equation (2-6) for full-scale solution gas flares. The results with natural gas from Howell et al. [2003] are reproduced in Fig. 5.

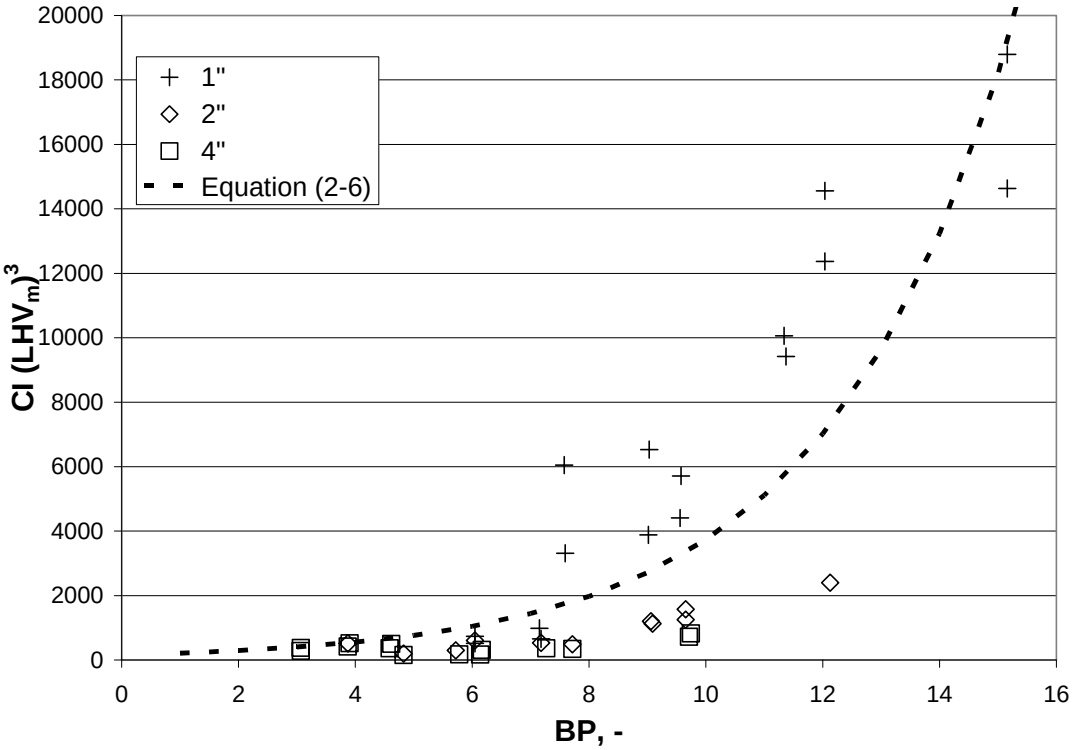

Figure 5 - Reproduction of Figure 6 in Howell et al. [2003].

These data are transformed into CI and replotted in Fig. 6 with a log-linear scale to better distinguish the effect of pipe size. There are ±100% bands put on equation (2-6). It is clear that the combustion inefficiency with 2.5 cm (1") pipe is significantly higher than with the 10.2 cm (4") pipe. The combustion inefficiency for the 10.2 cm (4") pipe is uniformly less than 1% (greater than 99% combustion efficiency) in these tests. This may indicate a minimum flare diameter around 7.6 cm (3") for wind-dominated

operation, as with the no-wind operation noted above. Certainly, equation (2-6) does not apply to flares larger than 2.5 cm (1").

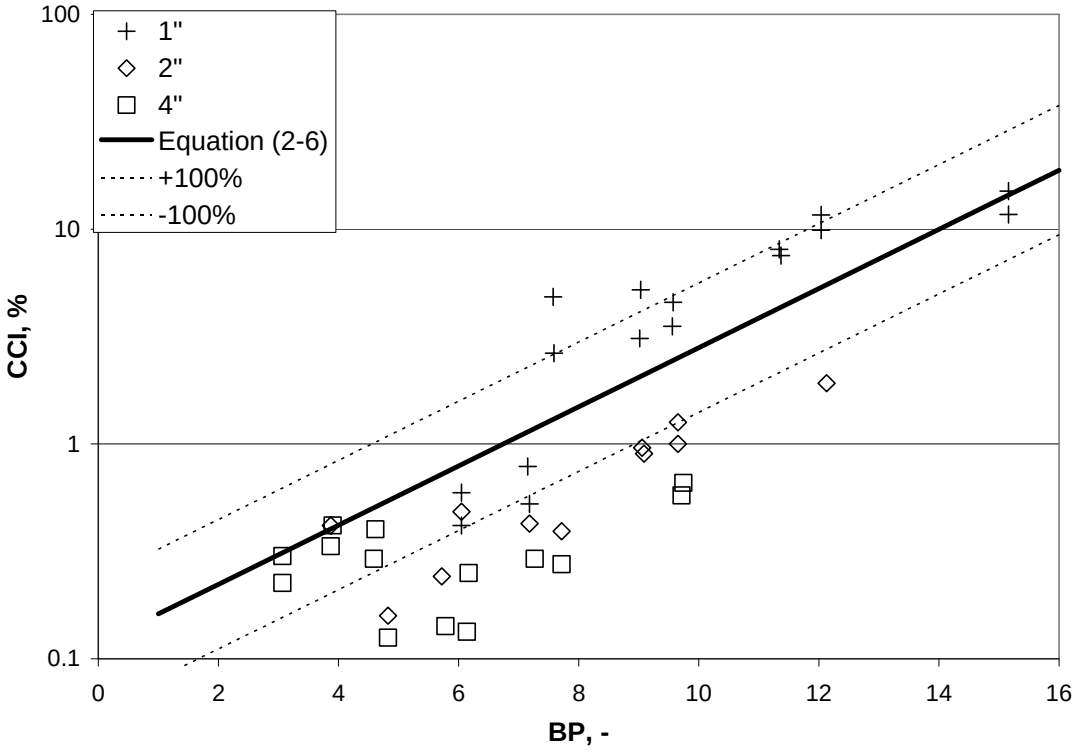

Figure 6 - The data from Figure 5 recalculated to give the combustion inefficiency (CI) and put ±100% bands on equation (2-6). Log-linear plot allows the data for the different pipe sizes to be easily distinguished.

A program of investigation with similar scope to that of the University of Alberta was started at the CanmetENERGY Flaring Test Facility (CanmetENERGY FTF) (Gogolek et al. 2001). A single pass wind tunnel was fabricated for this work. Natural gas and propane were fired, singly and in mixtures. Nitrogen and carbon dioxide were used as inert diluents. Pipe sizes from 2.5 cm to 15.2 cm (1" to 6") were used. Different configurations of wind shroud were tested, as was the effect of cross-wind turbulence. Again, it is important to reiterate that these tests were targeted at understanding the performance of small and simple solution gas flares.

Wind was shown to have a strong effect on combustion efficiency. They verified the importance of the ratio $U_w / U_f^{1/3}$ to correlate the CI values. However, a different dimensionless parameter was constructed. It is the ratio of the power of the cross-wind to

the power of combustion of the flare gas. The cube root of this ratio was called the Power Factor, PF, and takes the form

$$PF = \left(\frac{\rho_a U_w D_p^2}{\dot{m}_f LHV_m} \right)^{1/3} = \left(\frac{\rho_a U_w D_p^2}{\rho_f A_p U_f LHV_m} \right)^{1/3} . \qquad (2\text{-}7)^1$$

This factor written in the second form is independent of pipe size.

The data from the CANMET FTF studies and the University of Alberta studies with the larger pipe sizes are directly comparable. Tests results for simple pipes of diameter 2.5 cm, 5.1 cm, and 10.2 cm (1", 2" and 4"), firing natural gas are available from the FTF to compare to the results from Fig. 6. Figure 7 shows the data for the 2.5 cm (1") pipes. The range of the buoyant plume parameter does not overlap, but the FTF data maybe a plausible extrapolation if the lowest efficiency U of A data is neglected (Kostiuk et al, [2004]).

1 At first glance, the Power Factor is not obviously dimensionless. In the second form, the units of the density terms cancel, as do the units of diameter squared with the open area of the pipe. The units of the lower heating value (mass basis) are J/kg = N m/kg = (kg m/s2) m/kg = m2/s2, which are the same units as for velocity squared. So it is dimensionless.

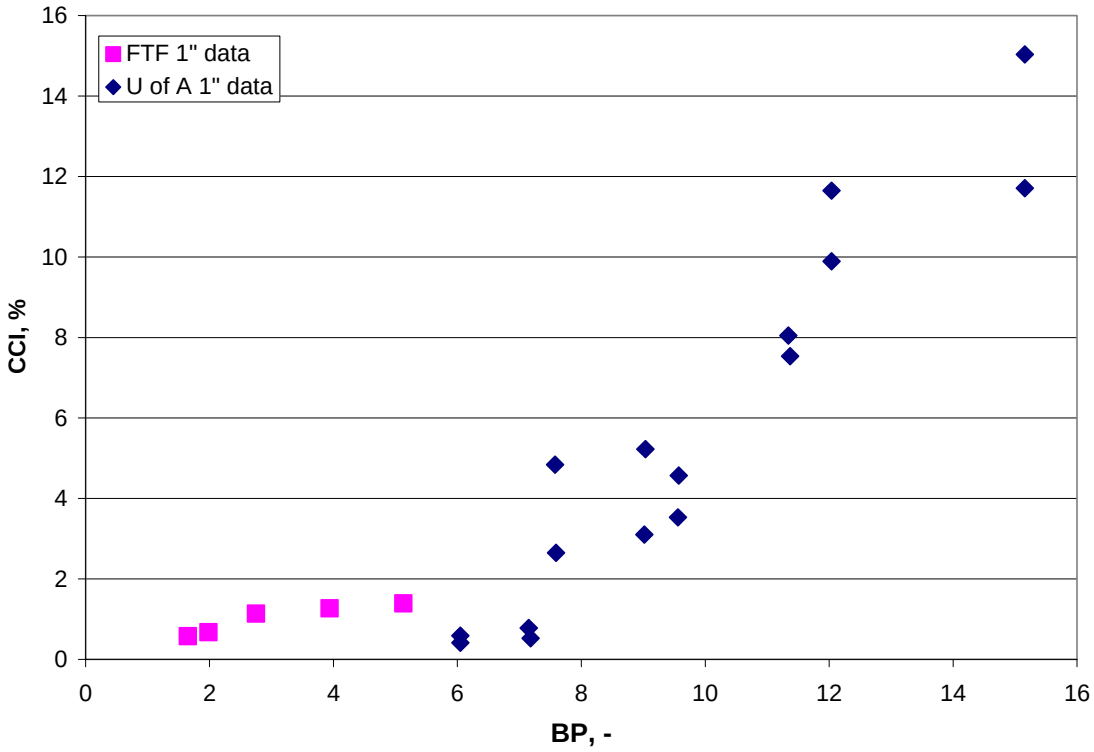

Figure 7 - Comparison of the combustion inefficiency results for 2.5 cm (1") pipe firing natural gas from the large-scale University of Alberta tests with those from the CanmetENERGY FTF, plotted against the buoyant plume parameter (equation 2-5).

Figure 8 shows the data for the 5.1 cm (2") pipes and Fig. 9 shows the data for the 10.2 cm (4") pipes. There is no significant discrepancy between the data from the two facilities.

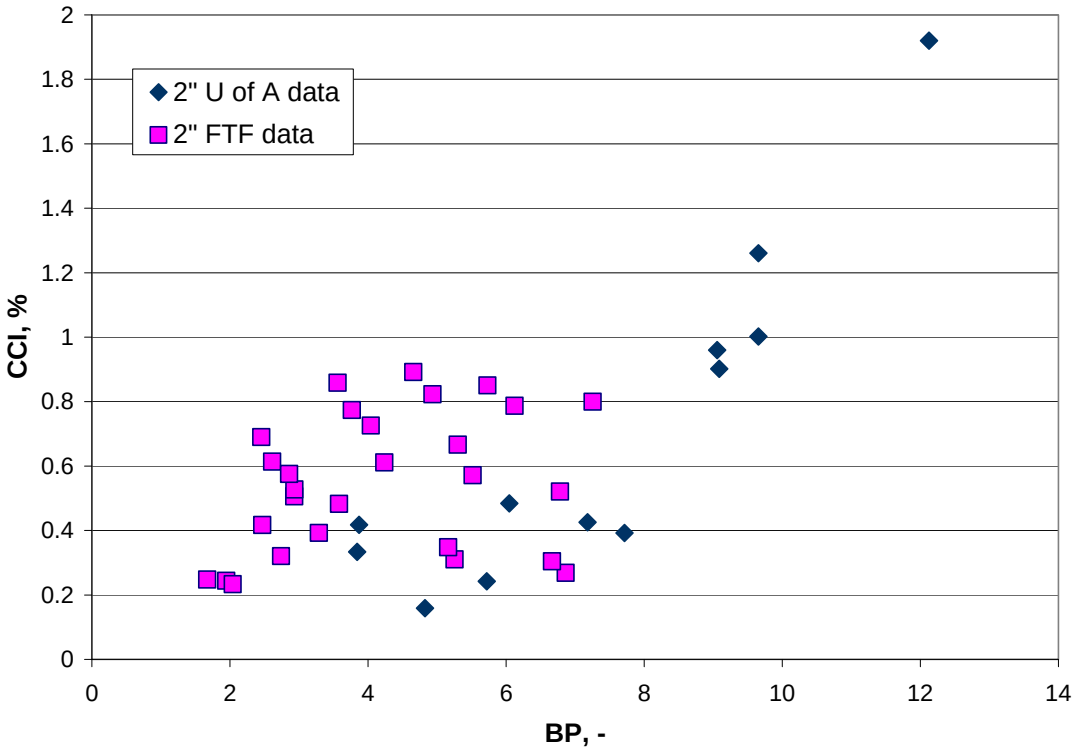

Figure 8 - Comparison of the combustion inefficiency results for 5.1 cm (2") pipe firing natural gas from the large-scale University of Alberta tests with those from the CanmetENERGY FTF, plotted against the buoyant plume parameter (equation 2-5).

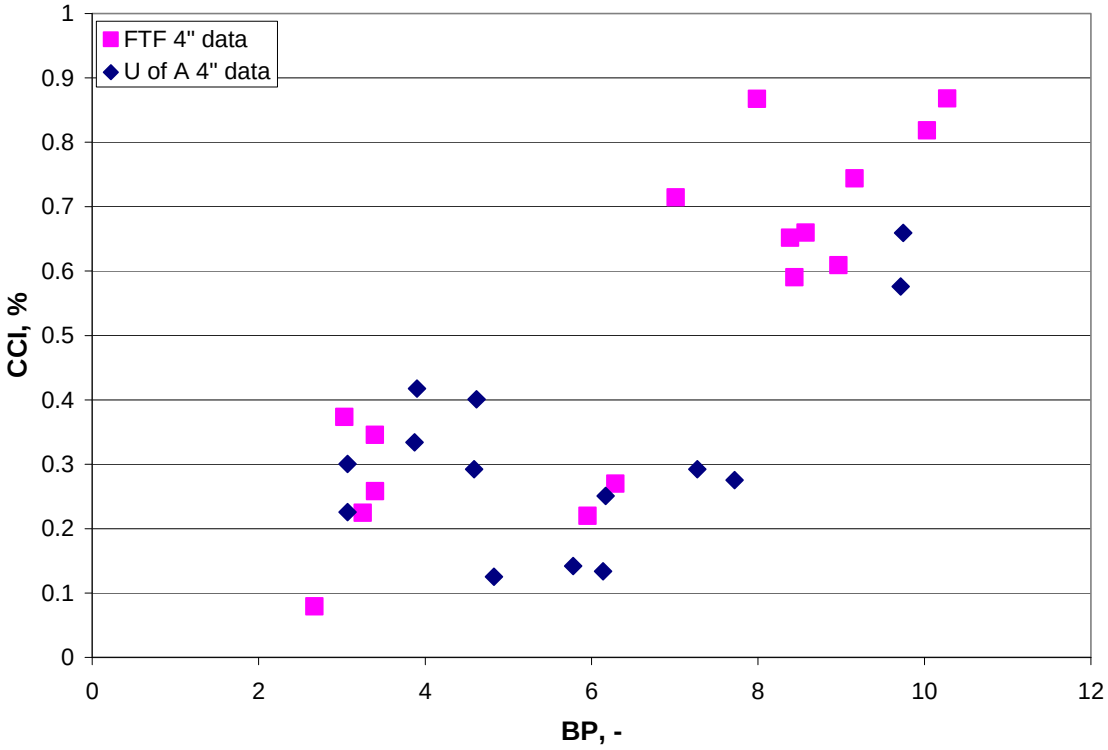

Figure 9 - Comparison of the combustion inefficiency results for 10.2 cm (4") pipe firing natural gas from the large-scale University of Alberta tests with those from the CanmetENERGY FTF, plotted against the buoyant plume parameter (equation 2-5).

Gogolek and Hayden [2004] reported tests firing natural gas diluted with nitrogen or carbon dioxide. Although the mixtures had the same heat content, on a volume basis, the natural gas/CO_2 mixtures had significantly lower CE relative to the natural gas/N_2 mixtures. Figure 10 shows the combustion inefficiency data for 60% diluent (15 MJ/m^3 or 400 Btu/scf) with varying wind speed.

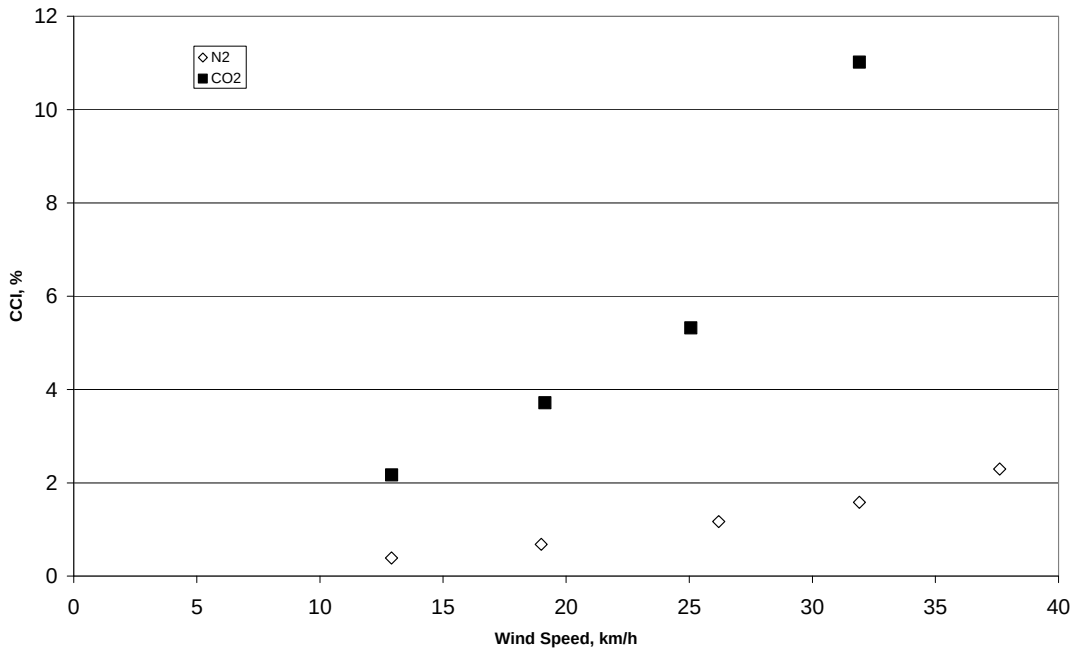

Figure 10 - Combustion Inefficiency for natural gas diluted with 60%-vol nitrogen and carbon dioxide, 10.2 cm (4") pipe. The flame blew out at the top wind speed of 43 km/h (27 mph) with carbon dioxide dilution. Data from Gogolek and Hayden [2004].

Gogolek and Hayden [2004] showed that grid turbulence can produce a significant decrease in combustion efficiency. Turbulence may be an important factor for solution gas flares that are on the order of 10 m (33') high, often in rough terrain. Grid turbulence is produced in a wind tunnel by placing a rigid uniform grid in the flow. This produces nearly homogeneous turbulence with length scales related to the grid structure. It is not clear whether the small-scale turbulence of these experiments is relevant to the large-scale turbulence experienced by tall industrial flare stacks.

Recently, open-path FTIR has been used for remote measurement of emissions from operating full-scale flares. Haus et al. [1998] reports FTIR measurements on three large natural gas flares with ambient winds speed about 16-24 km/h (10-15 mph). In six tests the combustion efficiencies averaged 99.3% and in all cases were >98.8%. Ozumba and Okoro [2000] reports tests conducted on 8 large natural gas flares of varying designs and flow rates. Direct measurements of combustion efficiencies were obtained by employing open-path Fourier transform infrared spectrometer (OP-FTIR) techniques. In variable

light wind conditions, all eight flares tested were found to have combustion efficiencies >98%. Similarly, Blackwood et al. [2000] reports OP-FTIR measurements on two "very large" (unspecified) flares in which the gas was approximately 99% carbon monoxide with the remainder being saturated water vapor, hydrocarbons and sulfur gases; i.e., a "very low-Btu" (unspecified) flare. In nineteen tests the combustion efficiencies averaged 98.2%.

Mellqvist [2001] reports the results of a remote sensing technique, Solar Occultation Flux, which uses the absorption spectra in the infrared of the plume with respect to solar radiation. He used this technique to measure the ethylene in the plumes from operating refinery flares. Wind speed was from 4 m/s to 7 m/s. The ethylene concentration in the flare gas ranged from 4%-v to 20%-v. He found destruction efficiency better than 97% when firing at full load (high flow rate of gas and high ethylene concentration). However, there were other conditions that produced destruction efficiency between 90% and 97% and destruction efficiency was from 50% to 90% at part load (less than 20% of full-load). This he attributed to over-steaming (SFR>2.5) and low ethylene concentration in the flare gas, as well as the low flare gas flow rate. He noted that the co-variation of operating conditions (flare gas flow rate, ethylene concentration, steam rate) which makes identification of the effects difficult. This is the general problem with field tests.

However, a blind test of an open-path passive FTIR (PFTIR) system left room for doubt about the accuracy of the technique (URS [2004]). A heated gas mixture simulating combustion products from an operating flare was sent up a stack. The remote sensing technique was not able to provide accurate measurement of the main combustion product (CO_2) or the trace hydrocarbon emissions that were the main target. They concluded that more work was needed to develop the technology for flaring applications. The URS study in 2004 evaluated the ability of the PFTIR to measure concentrations of simulated flare emissions. It was concluded that PFTIR is a potentially viable technology for characterizing flare emissions. Controlled flare burning efficiencies were 99.5-99.9% when burning propane. Further tests were recommended to be done on the simulated flare and an actual flare. Another blind test of an open-path FTIR system concluded that PFTIR is a potentially viable measurement technique, but additional testing would be needed to determine PFTIR's suitability to measure flare efficiency. This further testing

should include hardware and analytical method refinements on the simulated flare prior to testing an actual flare.

We have outlined the difficulties in making remote sensing work in the introduction. It is worth listing them here:

- Concentration, temperature, and velocity profiles are not known *a priori*.
- There can be spatial and temporal fluctuations of velocity and concentration.
- Deconvolution is possible, e.g. tomography, but only if the time for data gathering (traverses) is shorter than the time scale of the fluctuations.
- Ambient conditions can cause significant interference with the measurement.

2.2 Published Work Conclusion

All studies, beginning even before those of the early-to-mid-1980s, including the most recent full scale remote sensing field tests, have consistently demonstrated the high efficiency of properly designed and operated industrial flares. Stable flare flames and high (>98-99%) combustion and destruction efficiencies are attained when the flares are operated within operating envelopes specific to each flare head and gas mixture tested. Operation beyond the edge of the operating envelope results in rapid flame de-stabilization and a decrease in combustion and destruction efficiencies. Flare flame stability and combustion efficiency may vary depending on flare head size, design, gas composition, and operating conditions include wind. Exceptions result when, for example, the flares are subjected to liquid carryover, or to over-steaming or to over-aeration; or in an effort to establish the limits of so-called "proper operation" are purposely tested at the verge of extinction.

Flare diameters used in EPA/CMA/EER testing and University of Alberta testing were small diameter pipe flares that may not be representative of industrial flare efficiencies. Testing efficiency of industrial flares that have much larger diameters is difficult if not impossible using classical source sampling methods. Remote sensing offers the possibility of measuring industrial size flares, but this method itself has some deficiencies that need further testing for validation.

It is important to keep in mind that no direct validation of remote-measurement techniques against reliable extractive sampling results has been carried out to date. The results of the few remote sensing field tests reported to date on real industrial flares in real plants under real ambient conditions seem to agree with the earlier flare efficiency studies. These showed combustion efficiency greater than 98% for properly designed industrial flares under normal operating conditions.

Any remote field testing to be carried out in the future should include a focus on the issue of wind. Moderate crosswinds have been shown to increase the efficiency of industrial flares by enhanced mixing but it has more recently been shown that strong crosswinds can have deleterious effects on flare efficiency in some circumstances. In addition, while the stability of large flares is well known to exceed that of small laboratory-scale model flares, the stability-scaling physics and chemistry are poorly understood. This important aspect, too, deserves emphasis in any testing to be taken up in future years.

In short, over the years it has become apparent that the efficiency argument resolves itself into what it means to be "properly designed and operated" and whether or not the EPA's 40CFR60.18 General Requirements for Flares that were intended to ensure “proper design and operation" do in fact ensure the high-efficiency operation of industrial flares.

3.0 ANALYSIS OF MAJOR VARIABLES AFFECTING PERFORMANCE

The major variables affecting flare performance are;

- Composition of flare gas.
- Flowrate of flare gas.
- Wind speed.
- Steam or air rate for assisted flares.
- Flare tip size.
- Flare tip design and configuration.
- Flare tip exit velocity.
- Pilot stabilization.

The effects of these are examined individually in this section. The issue of scale-up is also addressed.

3.1 Fluid Mechanical Regimes

This discussion concerns only unassisted flares. The fluid mechanical effect of steam-assist is to increase the flare gas momentum, moving towards or further into the jetting regime.

There are three clearly identified regimes for the flow regimes for elevated flares:

- *Jetting* – flow dominated by inertia of flare gas leaving the flare tip.
- *Wake-stabilized* – flow dominated by crosswind, with the flare flame anchored in the wake of the flare tip.
- *Buoyant* – low wind, low flare gas exit velocity, with the flow dominated by the buoyancy of the hot combustion gases.

The flare's physical design characteristics and flow regime determine the mixing behaviour between the air and flare gas, which is important for combustion. The following discussion considers the simple pipe flare, which is typical of those used in published studies. Correlations for efficiency of assisted (air or steam) flares will be discussed later in this section.

When attempting to correlate flare efficiency with fuel properties, it is important not to confuse mixing regimes. The mixing in a flare flame, with the possible presence of a crosswind, will depend on the air and fuel properties, average speeds and pipe size. From these flow variables one can form two dimensionless parameters representing the relative strength of the momentum fluxes. One is the Froude Number

$$Fr = \frac{\rho_f U_f^2}{(\rho_a - \rho_p) g D_p} \tag{3-1}$$

the ratio of the jet strength to the buoyancy of the burned gases. The other is the momentum flux ratio

$$R = \frac{\rho_f U_f^2}{\rho_a U_w^2} \tag{3-2}$$

which gives the relative momentum strength of the fuel jet to the crosswind. A rough regime map based on these two parameters is given in Fig. 11.

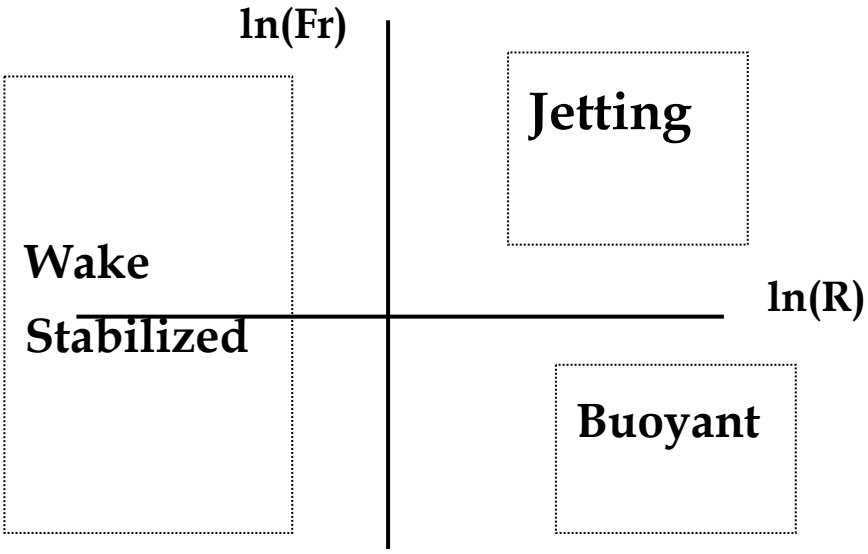

Figure 11 - Schematic regime map of fluid mechanical behaviour for elevated flares.

The wake-stabilized regime is established for $R \leq 0.1$. The jetting regime is for $R \geq 10$ and $Fr > 10$. The buoyant regime is for $R \geq 10$ and $Fr < 0.1$. These are notional boundaries and are not to be taken as definitive.

The properties of the jetting regime were examined in the authoritative review of Joseph et al. [1983]. The basic behaviour for simple jet is as follows: the jet entrains the surrounding air needed for combustion; the jet turbulence mixes the air and the flare gas; the jet can extinguish the flame as a result of high strain rates due to large velocity gradient around the perimeter of the jet. As the jet velocity increases and approaches the flame speed, the flame will tend to lift. Lifting of the flame away from the flare pipe is called *blow-off*. If the flame is extinguished, it is called *blow-out*. A *lifted flame* is one that has blown-off but not blown-out.

A strong jet in a moderate crosswind, such that $R \geq 10$, increases the entrainment of air into the jet. As the jet slows, the wind pushes the jet downwind. Also, the jet near the pipe tip acts as an extension of the pipe so that a wake develops on the downwind side of the jet. This wake is a zone of lower pressure, and it pulls the jet downwind. The buoyancy of the hot combustion products always increases the vertical momentum. The

trajectory of the flame is the result of the lift from buoyancy, the push from the wind and the pull from the low pressure in the wake.

The buoyant regime has very low initial flare gas momentum. At lower gas exit velocities, air will primarily be drawn to the flame by the buoyancy of the heated products of combustion. A buoyant flame is typically softer, longer and more wind affected (thought still stable) than a flame that uses higher gas exit velocities.

The stability of lifted flames is a subject of recent academic research (Lyons 2007 is a review of the topic). A flare burner mixes fuel and air at velocities, turbulence and concentration required to establish and maintain proper ignition and stable combustion. A detached stable flame is a flame which is not in contact with the flare burner itself but burns with a stable flame front in the vicinity of the flare burner. For many years, industrial flares have been designed for stable operation with a lifted flame. However, in some pilot-scale testing (e.g., EER, 1997) lifting of the flame was considered as the onset of instability. This is one indication of the differences between pilot-scale studies and industrial practice.

Industrial flares often have air or steam assist, to control smoking. The simplest way of incorporating assist media into Equations 3-1 and 3-2 is to combine the flows of the flare gas and the assist media (air or steam). The numerators of R and Fr are the momentum flux of the flare gas. The momentum flux for the assist media can be added to give the total momentum flux at the flare tip. However, care must be taken because the assist media also change the mixing of air and flare gas which will change the combustion characteristics.

In the wake-stabilized regime the burning flare gas is pulled into the wake of the flare stack. The literature on smoke stack design and performance can provide some guidance (Johnston and Wilson 1997, Overcamp 2001, Tatom 1986, Robinson and Hamilton 1992). Smoke stacks studies have looked at the trajectory of hot, buoyant gases in a wind. The wake of a smoke stack will be similar to the wake of a flare stack.

Flow of wind across a structure exerts a force on the structure and creates a wake downwind. In the immediate wake, there are locked-in counter-rotating vortices. These

locked-on vortices can also occur in the immediate wake of a strong jet. As the wind increases the shedding of vortices occurs, creating the von Karman vortex street. The frequency of vortex shedding f_v changes with pipe size and wind speed. This frequency is a measure of the dynamics in the wake of the pipe. The Strouhal number ($St = f_v D_p / U_w$) is the dimensionless vortex shedding frequency and is plotted against the Reynolds number for a cylinder ($\mathrm{Re}_w = U_w D_p / \nu_a$) in Fig. 12.

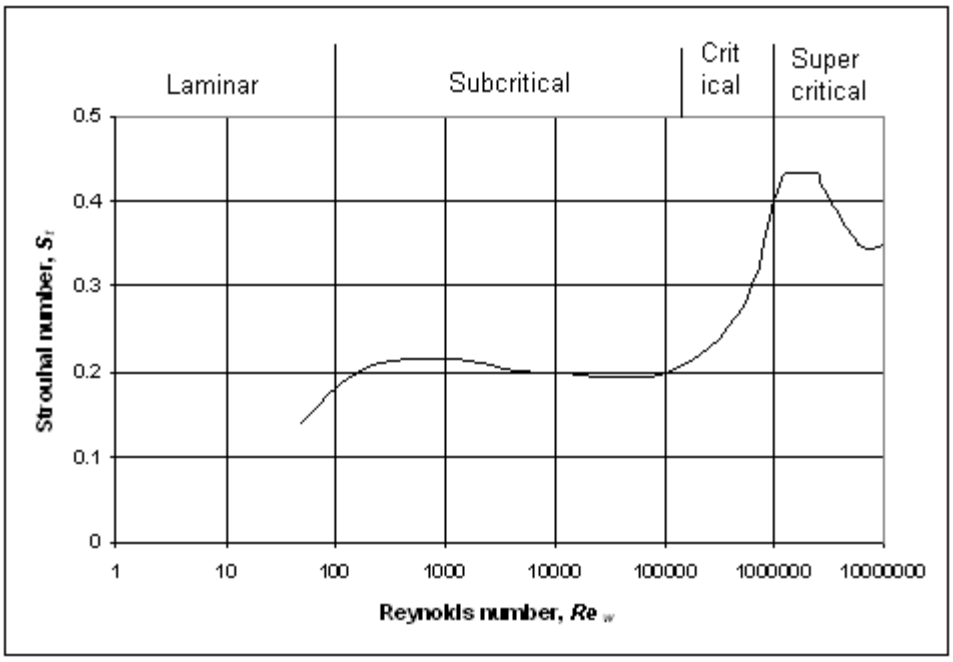

Figure 12 - Plot of Strouhal number for a cylinder against cross-flow Reynolds number.

The Strouhal number is almost constant at 0.2 for Reynolds numbers from 10,000 to over 100,000. The boundary layer thickness becomes turbulent for Reynolds number above 300,000. The flow is called sub-critical for Reynolds number below 300,000, critical for Reynolds numbers from 300,000 to 1,000,000. Above that, the flow is called super-critical.

There is a steady force (F_s) on the structure and a dynamic force (F_d) due to vortex shedding. The dimensionless coefficients for these forces are

$$C_d = \frac{F_s}{\frac{1}{2}\rho_a U_w^2}, \quad C_l = \frac{F_d}{\frac{1}{2}\rho_a U_w^2} \tag{3-3}$$

The drag coefficient, C_d, for a long cylinder is plotted against Reynolds number in Fig. 13. The drag coefficient is approximately constant for Reynolds number from 1000 to 100,000, with a minimum around $\mathrm{Re}_w = 300{,}000$. The dynamic force coefficient, C_l, is also plotted in Fig. 13. This coefficient has a maximum around $\mathrm{Re}_w = 70{,}000$ then decreases to a constant value for Re_w above 250,000.

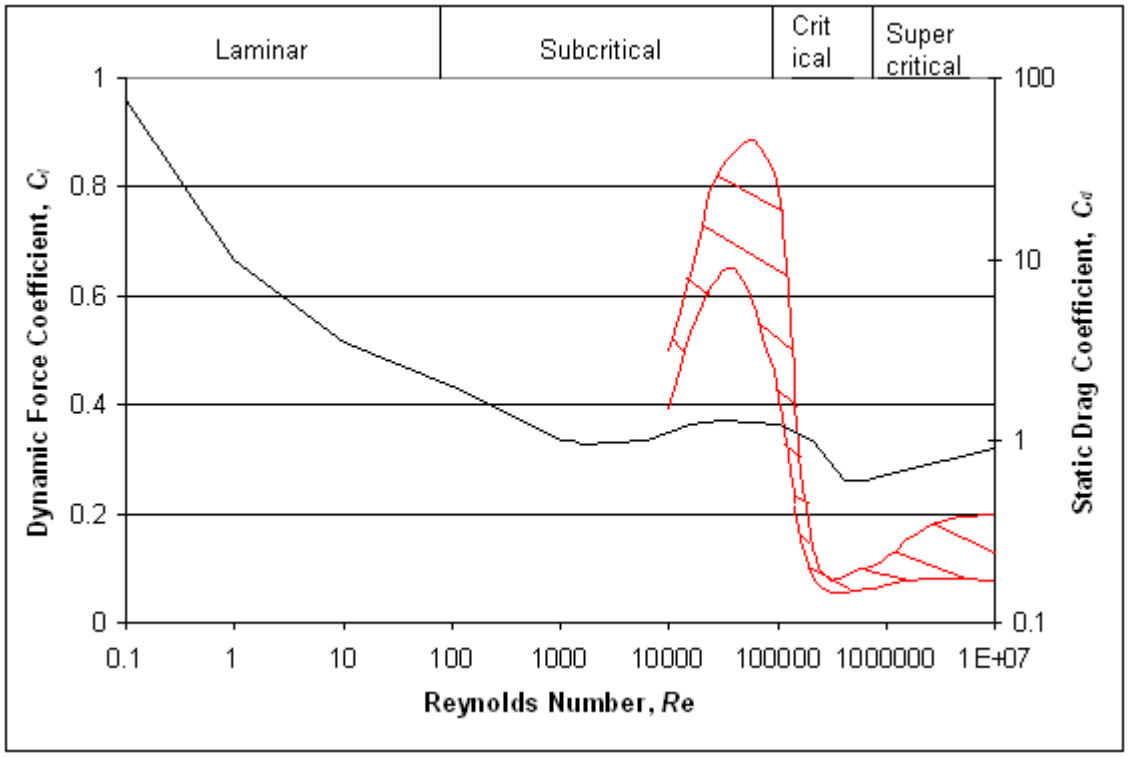

Figure 13 - Static drag coefficient and the dynamic force coefficient for a cylinder as a function of the crossflow Reynolds number.

Downwash is the phenomenon where the plume from the stack is pulled into the wake of the stack and the pollutants in the plume more easily reach ground level. Downwash has been shown to occur for a momentum flux ratio of $R < 2.5$ (Overcamp [2001] and Tatom [1986]) with the stack Reynolds number in the critical regime ($\mathrm{Re}_w > 100{,}000$), that is for large diameter stacks and moderate to high winds. Johnston and Wilson [1997] used the circulation of air over the stack to derive a semi-empirical model for the onset and

strength of the downwash. Of note for flare stacks is the appearance of a modified wind speed

$$U'_w = \frac{U_w}{1 + 0.38R} \tag{3-4}$$

This can be useful for correlating the effect of wind speed on flare performance. As the momentum flux ratio gets large (strong jet), the modified wind speed gets small, while small momentum flux ratio (weak jet) leaves the wind speed unchanged.

With these considerations, the effects of the major variables on flare performance and emissions have to be examined within the particular regimes, followed by the search for links between the regimes.

3.2 Flare Gas Composition

The flare gas composition for refinery flares can vary quite widely, from high heat content streams with high molecular weight from an aromatics unit, to hydrogen-rich refinery fuel gas, to natural gas for purging, or to inert-rich gas created during start-up and shut-down. For plant design, the full range of relief gas compositions and flare burner exit velocities must be engineered to operate successfully with the size of pipe flare selected. In this section we first examine qualitatively the effects of varying flare gas composition in the jetting and wake-stabilized regimes. This is followed by a discussion of the characteristics needed to produce a practical correlation of flare performance with gas properties. The section ends with an extensive examination of the mixture rules for flammability limits and laminar burning rate.

3.2.1 JETTING REGIME

Flare performance, as measured by the combustion efficiency or destruction efficiency, is directly related to stability in the jetting regime. The determination of stability is done by visual observation of the flame which depends on the luminosity of the flame and may be subjective. The measured inefficiency is purely objective and quantified and is the preferred method of determining stability. The maximum exit velocity is determined by the flare gas properties. That there is a rapid, almost discontinuous decrease in efficiency

in the jetting regime as the exit velocity approaches its maximum was shown in the EPA-funded tests of the 1980s (Pohl et al. 1985, Pohl and Soelberg 1985, 1986).

This maximum stable velocity is decreased by an increase in the inert content of the gas, with carbon dioxide producing a greater decrease than nitrogen, at the same volumetric dilution level. Increased inert content of the gas also decreases the luminosity of the flame, making the determination of instability more difficult. Relatively small amounts of hydrogen, ~ 10%-vol., significantly increase the maximum stable exit velocity, and guarantee greater than 98% destruction efficiency for small amounts of hydrocarbon in nitrogen in an unassisted flare.

Steam-assist acts to reinforce the jet momentum. It also acts to dilute the flare gas by the introduction of steam and entrained air. This dilution effect is discussed more within the topic of flammability limits. Steam-assist is used to prevent smoking of the flare. The tendency of the flare gas to smoke is related to the molecular structure of the hydrocarbons present, often summarized by the molecular weight and H:C weight ratio. The steam-to-fuel ratio (SFR) is the mass of steam injected to the mass of flare gas. This is the total amount of flare gas, not simply the amount of hydrocarbon. The amount of steam-assist required to prevent a flare from smoking is related to the tendency of the fuel to smoke. The tendency to smoke is roughly correlated with the weight ratio of hydrogen to carbon. Table 4 gives a number of combustion properties of selected compounds and reproduces the suggested SFR to prevent smoking for a variety of hydrocarbons (API Standard 521, Table 11). The optimal SFR will vary with flare type and design.

Table 4 - Combustion properties of selected combustible gases [Source: Baukal and Schwartz (2001)] and suggested range of steam-to-fuel ratio (SFR) from API Standard 521, Table 11.

	Density	LHV		Air:Fuel		S_{st}	LFL	UFL	SFR
Species	**kg/m^3**	**MJ/m^3**	**MJ/kg**	**vol/vol**	**kg/kg**	**cm/s**	**%**	**%**	**kg/kg**
CH_4	0.68	37.6	55.4	9.55	17.20	40.5	5	15	-
C_2H_6	1.27	66.0	51.9	16.71	15.90	42.5	3	13	0.1 – 0.15
C_3H_8	1.87	94.0	50.4	23.87	15.25	44	2.1	9.5	0.25 – 0.3
C_2H_4	1.19	59.7	50.3	14.32	14.81	66	2.75	34	0.4 – 0.5
C_3H_6	1.78	87.1	48.9	21.48	14.81	70.2	2	10	0.5 – 0.6
H_2	0.085	12.1	142.0	2.39	34.29	210	4	74.2	-
CO	1.19	12.0	10.1	2.39	2.47	28.5	12.5	74.2	-
H_2S	2.72	22.2	15.2	7.16	6.09	39.1	4.3	45.5	-

3.2.2 BUOYANT REGIME

The buoyant regime has gained greater significance as flare gas reduction projects have been implemented. Lower quantities of flare gases are being sent to flares. In the absence of wind, combustion efficiency is above 98% until the blow-off velocity is approached, at which point the flare is operating in the jetting regime. With wind present, buoyant operation moves directly to wake-stabilized operation.

3.2.3 WAKE-STABILIZED REGIME

In contrast to the jetting regime, the wake-stabilized regime displays a continuous decrease in flare performance as the flare gas inert content increased, until extinction. Studies in this regime (at University of Alberta and CanmetENERGY) fired models of associated gases, namely the lighter alkanes – methane, ethane and propane. The efficiency of flares firing natural gas (mostly methane) degrades most easily. The efficiency of flares firing ethane or propane displays similar behaviour. Increased content of either nitrogen or carbon dioxide in the flare gas decreases efficiency. Carbon dioxide has a much stronger effect than nitrogen for the wake-stabilized regime, as observed in the jetting regime.

3.3 Combustion Properties of Gas Mixtures

Most studies of flare performance used relatively pure combustible gas or a binary mixture of a fuel gas with a single inert gas. In practice, the flare of a refinery must handle different mixtures of many gases. A correlation of flare performance with flare gas properties can be developed for pure gases or binary mixtures, but to be useful the correlation must be applicable to the complicated mixtures of actual practice. Therefore, the combustion properties used in the correlation must have the following characteristics: (Pohl et al. [2004])

- They must be clearly defined.
- They must be tabulated for a wide range of compounds, or directly calculable from tabulated properties of a wide range of compounds.
- There must be unambiguous mixing rules for each property that includes the treatment of inert gases.

A variety of different fuel properties have been used or proposed to correlate performance of flares. These include

LHV_v – net heat content on a volume basis (i.e. with water as a vapour in the combustion products).

LHV_m – net heat content on a mass basis.

$S_{\max}$ – maximum laminar flame speed or burning rate.

LFL, UFL – lower and upper flammability limits, vol-%.

T_{ad} – adiabatic flame temperature.

SA_m, SA_v – stoichiometric air-to-fuel ratio, mass basis or volume basis.

Table 4 has these properties for a selection of gases commonly fired in flares. It is clear that the first two of our required characteristics are met for all these properties of the combustible gases. The following combinations have been used in the literature to correlate blow-off velocity, or maximum stable exit velocity.

$$\frac{LHV_v}{\dot{Q}(1500^\circ C)}\frac{UFL}{LFL} \qquad \text{Noble et al. [1984]} \qquad (3\text{-}5)$$

$$\frac{100\% - LFL}{LFL}\frac{\rho_f}{\rho_a} \qquad \text{Shore [2007]} \qquad (3\text{-}6)$$

$$\mathrm{Re}_f = \frac{H_f S_{\max}}{\nu_f} \qquad \text{Kalghatgi [1981a and b]} \qquad (3\text{-}7)$$

Johnson et al. [2000] used the maximum dilution ratio, which is derived from the lower flammability limit, and maximum flame speed to correlate the inefficiency of natural gas/carbon dioxide mixtures in the wake-stabilized regime. However, this correlation was discarded in subsequent papers in favour of the heat content on a mass basis.

3.3.1 MIXING RULES

The remaining characteristic is the mixing rule. The gas composition is given by x_i, the volume fraction of component i, or w_i, the mass fraction of component i. The adiabatic flame temperature is calculated from heat balance of heat released by combustion with the enthalpy of the products. This calculation is straightforward. The mixing rules for heat contents, stoichiometric air and density are

$$LHV_{v,mix} = \sum_i x_i LHV_{v,i} \qquad (3\text{-}8)$$

$$LHV_{m,mix} = \sum_i w_i LHV_{m,i} \tag{3-9}$$

$$SA_{mix} = \sum_i x_i SA_i \tag{3-10}$$

$$\rho_{mix} = \sum_i x_i \rho_i \tag{3-11}$$

3.3.2 MIXING RULE FOR FLAMMABILITY LIMITS

The mixing rule for flammability limits is a little more complicated. Le Chatelier's principle states that the air-to-fuel ratio of a mixture of combustible gases at the flammability limit is equal to the volume-fraction weighted sum of the air-to-fuel ratio at the flammability limit of each component. In symbols this is

$$\frac{100 - FL_{mix}}{FL_{mix}} = \sum_i x_i \left(\frac{100 - FL_i}{FL_i} \right) \tag{3-12}$$

This reduces to

$$\frac{1}{FL_{mix}} = \sum_i x_i \left(\frac{1}{FL_i} \right) \tag{3-13}$$

This rule applies to both upper and lower flammability limits, and when all the components are flammable. It has proven successful in most cases, although there is significant deviation with sulphur-bearing compounds like hydrogen sulphide in the mixture.

The treatment of inert components in Le Chatelier's principle is problematic. For binary mixtures of fuel gas with nitrogen or carbon dioxide there are the flammability diagrams found in Zabetakis [1965]. An extensive collection of flammability data is also found in Coward and Jones [1952]. The diagram for methane/nitrogen and methane/carbon dioxide binary mixtures is reproduced in Fig. 14. However, the method with multiple combustible components is not clear. Zabetakis recommends assigning the inert component(s) to a single combustible component, using the flammability diagram for that binary mixture, and then treating the binary mixture as a single combustible component with LeChatelier's principle (equation 3-13). Clearly this an *ad hoc* rule and it has been

shown that the calculated flammability limits can be significantly different depending on which pairings are used (eg., Karim et al [2004]). In addition, the amount of inert may exceed the flammable capacity of a single component. Further ambiguity is therefore introduced in dividing up the inert component among the combustible components.

An alternative method, at least for the lower flammability limit, is to treat all the inert components the same and to set $LFL_{inert} = \infty$. This zeroes the terms in equation (3-13) for the inert species. There is some evidence that this works for nitrogen (Karim et al [2004]), but clearly will not produce the observed difference between nitrogen and carbon dioxide, for example.

If we return to the original formulation of LeChatelier's Principle, equation (3-12), and assign an air-to-fuel ratio of -1 to nitrogen, and let the nth component be nitrogen, then (3-12) becomes

$$\frac{100 - FL_{mix}}{FL_{mix}} = \sum_{i=1}^{n-1} x_i \left(\frac{100 - FL_i}{FL_i} \right) - x_n \tag{3-14}$$

This simplifies to

$$\frac{1}{FL_{mix}} = \sum_{i=1}^{n-1} x_i \left(\frac{1}{FL_i} \right) \tag{3-15}$$

This is how the $LFL_{inert} = \infty$ result is obtained. For the simple binary mixture of combustible gas with nitrogen, this method gives the constant fuel fraction in the flammability diagram, as shown in Fig. 14 for methane, which is common for most fuel gases.

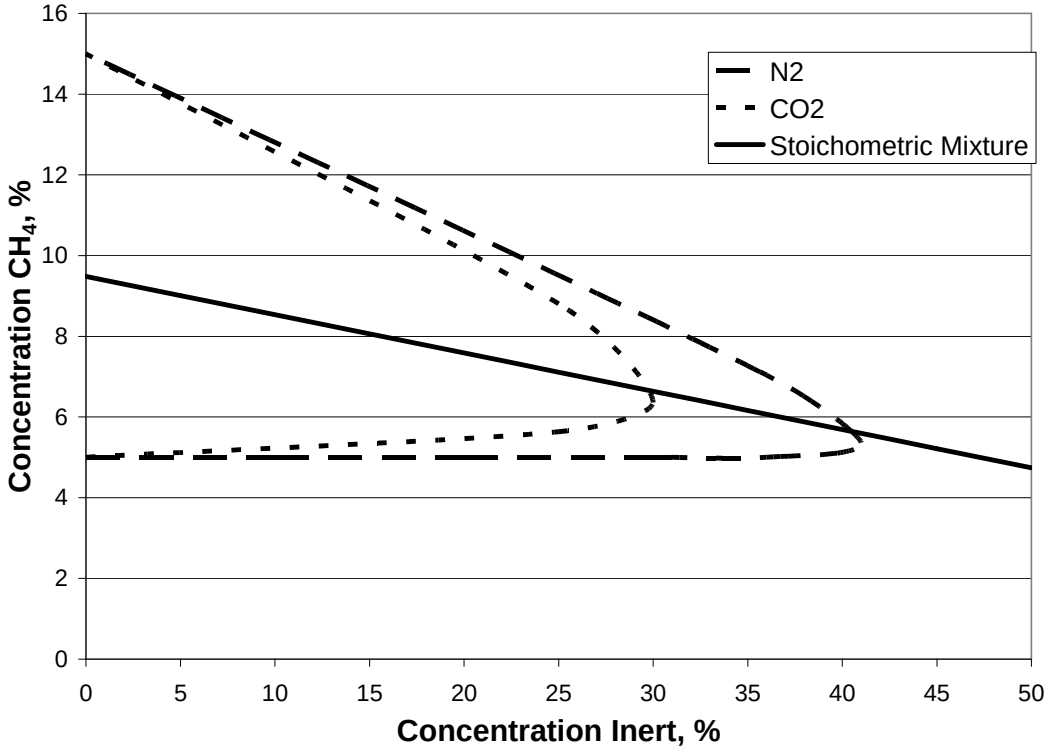

Figure 14 - Flammability diagram for methane, after Zabetakis [1965].

For other inert species, a nitrogen-equivalence factor N_e is assigned, which means an air-to-fuel ratio of $-N_e$ is used in equation (3-12).

$$\frac{100-FL_{mix}}{FL_{mix}} = \sum_{i=1}^{n-1} x_i \left(\frac{100-FL_i}{FL_i} \right) - N_e x_n \tag{3-16}$$

This simplifies in turn to

$$\frac{1}{FL_{mix}} = \sum_{i=1}^{n-1} x_i \left(\frac{1}{FL_i} \right) - (N_e - 1) x_n \tag{3-17}$$

This is the form of LeChatelier's Principle for an inert gas other than nitrogen. The recommended values of nitrogen equivalency have been tabulated by Molnarne et al. [2005] and selected values reproduced in Table 5.

Table 5 - Nitrogen equivalence values for carbon dioxide and water vapour reported in Molnarne et al. [2005], with values obtained by fit to flammability diagrams of Zabetakis [1965].

Species	CO_2	H_2O	CO_2 fit
CH_4	2.23	1.87	1.6
C_3H_8	1.93	1.51	2.5
C_2H_4	1.84	1.68	1.8
C_3H_6	1.92	1.36	2.4
H_2	1.51	1.35	1.5

The value of nitrogen equivalent factor varies with the combustible gas. This causes problems for choosing which value of nitrogen equivalence to use with a given mixture of combustible gases. Shore [2007] suggests using an average value of nitrogen equivalence, for example $N_e = 1.87$ for carbon dioxide. The ratio of specific heats of carbon dioxide and nitrogen is approximately 1.9, which is close to Shore's recommendation.

Karim et al [2004] measured the lower flammability limit for mixtures of methane and hydrogen with either nitrogen or carbon dioxide. Figure 15 shows the comparison of the experimental determination of lower flammability limit by Karim et al [2004] with the calculated limits using equation (3-17) with different values of nitrogen equivalence for carbon dioxide.

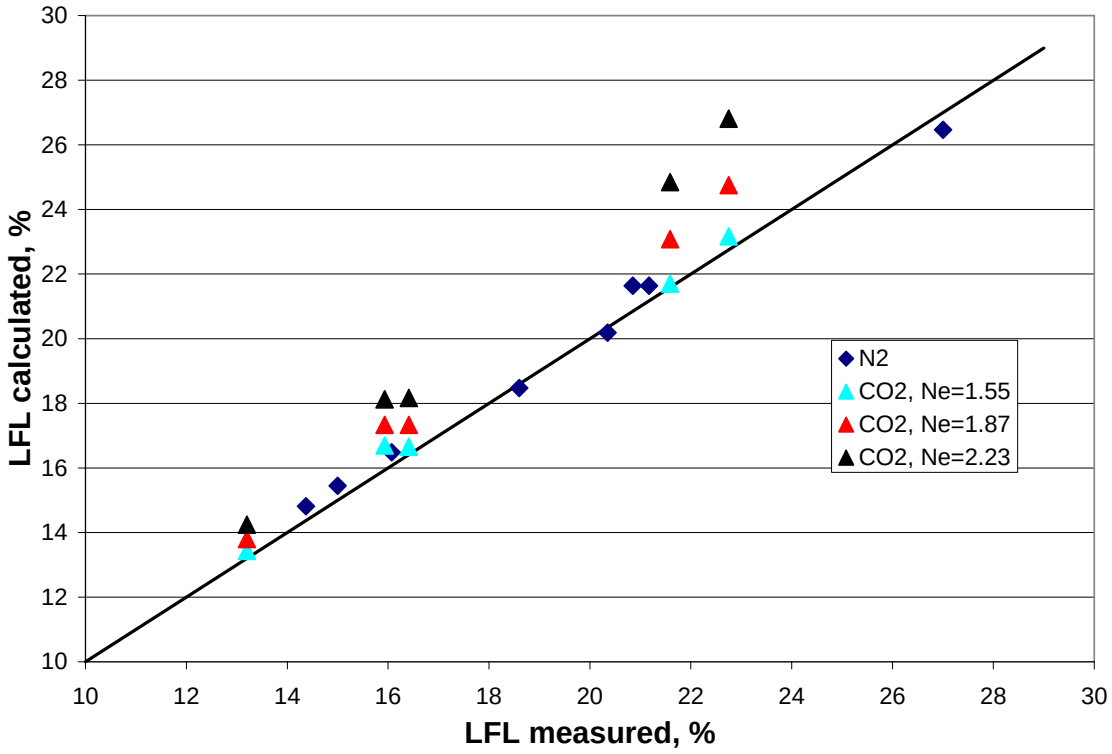

Figure 15 - Comparison of calculated lower flammability limit of methane/hydrogen/inert systems with measured lower flammability limit data from Karim, et al [2004]. Different values of nitrogen equivalence for carbon dioxide are used.

The methane/hydrogen/nitrogen data are fit well. The methane/hydrogen/carbon dioxide data are fit well with nitrogen equivalence of 1.55, the value for carbon dioxide with hydrogen, is much lower than the recommendations of Shore [2007] (1.87) or Molnarne [2005] (2.25) for carbon dioxide with methane. It is close to our value obtained by fitting the lower flammability data of Zabetakis [1965], reported in Table 5.

The flammability diagrams of Zabetakis [1965] can be used to establish nitrogen equivalence values for carbon dioxide for various combustible gases by finding the best fit using equation (3-17). These values are presented in Table 5. There are some significant differences between these values and those of Molnarne et al. [2005]. Of particular note, the value for methane is much lower while that for propane is much higher. The value for carbon dioxide with methane is the same as that for carbon dioxide with hydrogen. We would suggest that the proper assignment of nitrogen equivalence factor for an inert gas with a mixture of combustible gases is to use the volume-weighted average of the nitrogen equivalence factors of each component. This gives an

unambiguous method of calculating the lower flammability limit. Elaboration of this suggestion is beyond the scope of this report.

An adequate summary of the flammability diagrams of Zabetakis [1965] is provided by a three-segment piecewise linear fit. The lower flammability curve is approximated by a line from the lower flammability limit with no inert to the value at maximum dilution. A similar line is constructed for the upper flammability curve. There is a vertical segment joining the end points of each line. This is illustrated in Fig. 16 with the flammability diagram for methane.

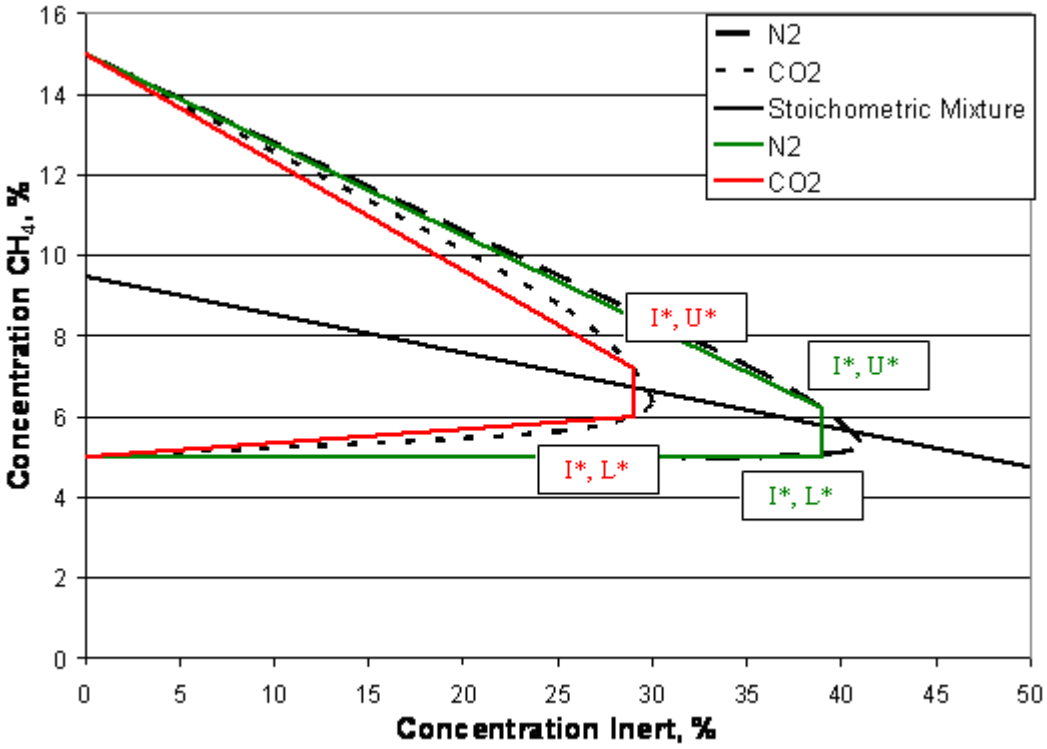

Figure 16 - Flammability diagram for methane with piece-wise linear representation given by the coloured lines.

This is a compact summary of the flammability diagram. The upper and lower flammability limits with the maximum dilution, lower limit fuel fraction and upper limit fuel fraction give the whole flammability diagram. These five values are given in Table 6 for a selection of fuel gases blended with nitrogen and carbon dioxide.

Table 6 - Tabulation of piece-wise linear representation of flammability diagrams for selected fuels diluted with nitrogen and carbon dioxide.

Species	LFL	UFL	Inert	I*	L*	U*
	%	%				
CH_4	5	15	N_2	39	5	6.2
			CO_2	29	6	7.2
C_3H_8	2.1	10.1	N_2	40	2.6	3.4
			CO_2	27	3.5	4.2
C_2H_4	2.75	28.6	N_2	45	2.6	5
			CO_2	40	3.7	5
C_3H_6	2	11.1	N_2	40	2.8	3.9
			CO_2	28	3.5	4.4
H_2	4	74.2	N_2	70	4	6
			CO_2	52.0	4.1	13

3.3.3 MIXING RULES FOR LAMINAR FLAME SPEED

The laminar flame speed, also called the laminar burning rate, is the rate of propagation of the flame interface into a uniform quiescent mixture of fuel and oxidant. It has a complex dependence on the rate of heat transfer from the flame to the unburned gas, rate of molecular diffusion of reacting species, particularly radicals, and the rate of heat generation by chemical reaction in the flame. It is a useful summary in a single parameter of the interplay of these rate processes. In the case of a flowing air/fuel mixture, the laminar flame speed has to match the local gas speed. If the flame speed is

higher, the flame propagates into the gas (flashback), while if the gas speed is higher the flame is carried away in the flow (blow-off).

Mixing rules have been proposed for the laminar flame speed by a number of researchers. Payman and Wheeler [1922] suggested a simple average, weighted by the volume fraction of the components. Spalding [1954] developed a mixing rule based on the weighted sum of the maximum rate of mass consumption, based on the heat transfer model of flame propagation. The rate of mass consumption is proportional to the square of the flame speed, so the Spalding mixing rule is a weighted sum of squares of flame speeds.

$$S_{mix}^2 = \sum_i \alpha_i S_i^2 \tag{3-18}$$

The coefficients are the mass fraction of fuel and air relative to the total mass of fuel and air in the mixture. The flame speeds have to be adjusted to the common flame temperature. The original formulation was ambiguous about how to assign the combustion air to the various fuel components. Inert components were incorporated in the model by reducing the mass fraction of the fuel (dilution) and lowering the common flame temperature. Yumlu [1967] tested the mixing rule against his own data for hydrogen/carbon monoxide/air flames. He found good agreement when the air was assigned to the fuel components to give the same equivalence ratio for each component. He determined the temperature dependence of the flame speed for hydrogen and carbon dioxide mixtures in separate experiments. He continued the work (Yumlu [1968]) with experimental determination of flame speed of methane with nitrogen addition. He found his modification of the Spalding mixing rule worked well for this binary mixture. Skrbić et al. [1985] tested several mixing rules on gas mixtures similar to natural gas. The mixing rules of Payman and Wheeler [1922], Spalding [1954] as modified by Yumlu [1967], and Harris and Lovelace [1968] were compared to their own experimental data. They also tested the effect of adding nitrogen and carbon dioxide. They found that the modified Spalding rule worked best. However, unlike Yumlu [1968], they had to include an additional term to account for the presence of inert gases.

More recently Hirasawa et al. [2002] proposed their own mixing rule, again based on the thermal transfer model of flame propagation. This rule combined flame speeds at the same equivalence ratio and gave very good results compared to their experimental data on binary mixtures of ethylene, n-butane and toluene in air. As formulated, this rule does not account for the presence of inert species. The starting point is the observation that the laminar flame speed has an Arrhenius dependence on flame temperature.

$$S = \exp\left(\frac{-\hat{T}_e}{T_{ad}}\right) \qquad \text{or} \qquad \hat{T}_e = -T_{ad}\ln(S) \tag{3-19}$$

Here $\hat{T}_e$ is a pseudo-activation energy temperature, but in fact is a lumped parameter including the heat transfer parameters and activation energy. T_{ad} is the adiabatic flame temperature. The mixing rule is based on the adjustment of the flame speed of each component from the respective adiabatic flame temperature to the flame speed at the common flame temperature. The mixing rule for the flame temperature is

$$T_{mix} = \sum_i \frac{x_i n_i T_{ad,i}}{n_{mix}} \tag{3-20}$$

The n_i are the number of moles of product from complete combustion of 1 mole of fuel at stoichiometric conditions and $n_{mix} = \sum_i x_i n_i$. The same mixing rule is applied to the pseudo-activation energy temperature for the mixture.

$$\hat{T}_{e,mix} = \sum_i \frac{x_i n_i \hat{T}_{e,i}}{n_{mix}} = \sum_i \frac{x_i n_i T_{ad,i}\ln(S_i)}{n_{mix}} \tag{3-21}$$

Applying these mixture temperatures to equation (3-19) and simplifying gives the following geometric mean of the component flame speeds.

$$S_{mix} = \prod_i S_i^{\vartheta_i} \quad \text{with} \quad \vartheta_i = \frac{x_i n_i T_{ad,i}}{\sum x_j n_j T_{ad,j}} \tag{3-22}$$

This formulation does not consider the inclusion of inert species in the mixture, since an inert species has neither an adiabatic flame temperature nor a laminar flame speed. A

formal procedure would be to include a different multiplier for each different inert species.

There are three papers (Scholte and Vaags [1959], Fells and Rutherford [1969], Skrbić et al. [1985]) that reported such multipliers for nitrogen and carbon dioxide. The three agree that the multiplier for the effect of nitrogen is

$$k_{N_2} = 1 - 0.8 x_{N_2} \tag{3-23}$$

There is significant discrepancy between the multipliers for carbon dioxide. They all have the same form as equation (3-23). The range is from

$$k_{CO_2} = 1 - 1.1 x_{CO_2} \tag{3-24a}$$

to

$$k_{CO_2} = 1 - 1.6 x_{CO_2} \tag{3-24b}$$

These data are all from methane-rich mixtures. The magnitude of the effect of carbon dioxide relative to nitrogen is similar to the magnitude of the nitrogen equivalence for the lower flammability limit.

3.4 Flare Gas Rate

3.4.1 JETTING REGIME

The exit velocity has already been identified as the determining parameter for the jetting regime. Maximum exit velocity is a function of the flare gas composition, as already noted.

Noble et al. [1984] used the Mach number as the dimensionless exit velocity. The Mach numbers for their data ranged from less than 0.1 to almost 1.

$$\frac{U_{f,\max}}{V_a} = 0.0008 \left[\frac{LHV_v}{\dot{Q}(1500^\circ C)} \frac{UFL}{LFL} \right]^4 \tag{3-25}$$

Shore [2007] did not render dimensionless the exit velocity in his correlation below:

$$\frac{U_{f,\max}}{\pi D_p} = 0.000066 \left[\frac{100 - LFL}{LFL} \frac{\rho_f}{\rho_a} \right]^5 \tag{3-26}$$

Kalghatgi [1981a] (see equation (2-1)) used the maximum flame speed to normalize the exit velocity. Note the very large exponents in equations (3-25) and (3-26). This makes the correlations very sensitive to small errors in the constituent parameters. For example, ±1% error in the lower flammability limit becomes ±4% in (3-25) and ±5% in (3-26); ±5% error in the lower flammability limit becomes (-18%, +23%) in (3-25) and (-22%, +29%) in (3-26).

As the inert fraction in the flare gas increases, the maximum stable exit velocity decreases. The wind speed necessary to move out of the jetting regime to the wind-stabilized regime is similarly decreased. There is no published information on the efficiency or emissions during the transition between the jetting and wake-stabilized regimes.

3.4.2 WAKE-STABILIZED REGIME

In the wake-stabilized regime, the wind is the dominant factor and the flare gas exit velocity is secondary. Both the University of Alberta and CanmetENERGY found that the combustion inefficiency is a function of the ratio $\frac{U_w}{U_f^{1/3}}$, so the effect of changes in the flare gas rate is rather weak. Increasing the flare gas exit velocity will increase efficiency, at least until the maximum stable exit velocity is approached.

3.5 Wind Speed

3.5.1 JETTING REGIME

Kalghatgi [1981b] studied the effect of wind on the blow-off velocity. He found that the maximum exit velocity, the blow-off velocity, increased with increasing wind. He also found that there was a minimum exit velocity, the blow-out velocity. This gave a region of stable operation. For a given fuel, scaling the exit velocity and wind speed with the pipe diameter collapsed all the results onto a single curve between the blow-out and blow-off velocities. Note, however, the pipes used in his work were 2.0 cm or smaller. We have already noted that the results from such small pipes do not scale-up. He did note the establishment of the wake-stabilized regime where there was no blow-out or blow-off, for low exit velocities. Unfortunately, he did not report any data for the low

wind speed and high exit velocity, an important transition regime. Shore [2007] has also indicated that the conditions described as blow off by Kalghatgi may be flame lift and not actual blow-off.

3.5.2 WAKE-STABILIZED REGIME

Wind sets up the wake-stabilized regime. This regime is characterized by the turbulent wake, which is a low-pressure zone that pulls the flare gas into the wake, and establishes the recirculating eddy locked to the pipe. Fuel stripping has been shown experimentally to be the major source of inefficiency in this regime. The University of Alberta correlated their results with an exponential function of their buoyant plume dimensionless group (equation 2-5). However, we showed in Figure 6 that this correlation doesn't work with their data for pipes greater than 5 cm (2"). The data for 10 cm (4") pipes, from both University of Alberta and CanmetENERGY, plotted in Fig. 9, shows a roughly linear dependence on the buoyant plume dimensionless group, which means a linear dependence on wind speed.

The atmospheric boundary layer is similar to the turbulent boundary layer familiar in engineering of pipe flow, having a defined friction velocity, roughness length, and the consequent log velocity profile. Most meteorological data on wind speeds are reported at the standard height of 10 m (33 ft), and the distribution of wind speeds is given by a Weibull distribution. These can be used with an efficiency curve with respect to wind speed to calculate an annual average efficiency. If the flare is operating continuously, which may be the case for some production flares, or if flaring episodes are randomly distributed, then the average efficiency is

$$\overline{\eta} = \int_0^\infty \eta(U_w)\, p(U_w) dU_w \tag{3-27}$$

In particular, if the efficiency curve is linear then

$$\overline{\eta} = \eta(\overline{U}_w) \tag{3-28}$$

That is, the average efficiency is the efficiency at the average velocity.

3.6 Steam Assist

The method of steam injection can range from simple high-pressure nozzles around the perimeter of the flare tip to multi-level exterior nozzles and internal steam addition, in many variations. The technology of steam addition is clearly important, but discussion of the details of the several designs is beyond the scope of this review.

The effects of steam injection in controlling smoking are threefold:

1. It entrains air into the flare gas to promote combustion and reduce pyrolysis of the hydrocarbon.
2. It adds hydrogen and oxygen to interfere chemically with the soot formation mechanisms.
3. It lowers the flame temperature since the steam acts as a heat sink for the heat released by combustion.

A given flare tip will have a maximum smokeless rating, for a given flare gas composition and pressure, and steam supply and pressure. The steam jets also increase the vertical momentum of the flare gas, entraining it as well as the ambient air. This increased momentum makes the flare flame more resistant to the effects of crosswind. Steam injection can also mold the flare flame and increase the stable operating envelope.

The suggested steam-to-fuel ratio (SFR) to eliminate smoking is less than one for most fuels (API Standard 521, Table 11), with pentadiene as an exception. These recommendations have no bearing on the destruction efficiency. What constitutes over-steaming, in the absence of wind, appears to be a SFR above 3.5. The CMA results (McDaniel [1983]) plotted in Figure 1 indicate that efficiency degrades with SFR above 3.5 when flaring propylene. Pohl and Soelberg [1984] similarly found efficiency above 98% for SFR below 3.5 with propane. However, both studies also has high efficiency (99.4%) with SFR over 100, but these conditions had very low flare gas flow rates and the pilot-burners provided the majority of the heat input.

The studies to date have not been evaluated for the effect of wind on a steam-assisted flare. The effect of steam-assist was not studied in DuPont's hydrogen flare work (EER, 1997). Siegel [1980] did look at steam-assist with hydrogen-rich flare gas, where the

hydrogen content was 40% or more. The minimum hydrogen content to guarantee 98% destruction efficiency with a steam-assisted flare has not been established.

The SFR has been used as the appropriate measure of steam-assist rate. However, there does not appear to have been a study published of whether it is a valid parameter for correlating combustion efficiency with steam-assist rates for a particular flare tip design.

3.7 Flare Diameter

It is easy to assign a diameter to the simple pipe flares that have been studied in the literature. The inner diameter is the important size for the jetting regime. Similarly, the outer diameter is the important dimension for the wake-stabilized regime. The effective diameter for a fuel jet is the actual diameter multiplied by the square-root of the density ratio

$$D_{eq} = D_p \sqrt{\frac{\rho_a}{\rho_f}} \tag{3-29}$$

This diameter would give an air jet with the same exit velocity and the same linear momentum as the fuel jet.

In the case of steam-assisted flares with a strong jet, the equivalent diameter can be defined as

$$D_{eq} = \frac{\dot{m}_{tot}}{\left(\frac{\pi}{4} G_{tot} \widehat{\rho}\right)^{1/2}} \tag{3-30}$$

This is the practice for steam-atomized heavy oil burners. The density used for burners is that of the combustion products at the flame temperature. For a steam-assisted flare, the temperature of 1500ºC (2732ºF) could be used, as in Noble et al. [1984].

3.7.1 JETTING REGIME

Kalghatgi [1981a,b] uses pipe diameter in the expression for the flame length. The blow-off velocity correlation without wind is quadratic in the flame Reynolds number, which means quadratic in the pipe diameter. It has a maximum at a flame Reynolds number of 140,000 and decreases to 0 at a flame Reynolds number of 290,000. This is clearly not the actual behavior,[2] illustrating the danger of extrapolating beyond the experimental conditions of a correlation. The other correlations of maximum exit velocity (Noble et al. [1984], Shore [2007]) are independent of diameter.

The work from the 1980's at EER (Pohl and co-workers [1984, 1985, 1986]) were able to place the data from 7.5 cm to 30 cm (3" to 11.8") pipes and commercial tips on the same stability curve of maximum exit velocity versus heat content for propane/nitrogen mixtures. This indicates that the maximum exit velocity is independent of pipe size, for sufficiently large pipes, that is to say, for 7.5 cm (3") or larger. However, this evidence applies only to unassisted flares; there is not similar evidence for steam-assisted or air-assisted flares.

[2] Hydrocarbon flare flames longer than 10 m (33') are frequently observed. The flame Reynolds number defined by Kalghatgi is above 300,000 for these flames, and the correlation predicts blow-off for these flames.

3.7.2 WAKE-STABILIZED REGIME

There is disagreement about the dependence of flare performance on pipe size in the wake-stabilized regime. The University of Alberta results with 2.5 cm (6.4") and smaller pipes show a dependence of efficiency on $D_p^{1/3}$ in the dimensionless buoyant plume parameter. However, including the results from larger diameter pipes, a better fit was obtained with $D_p^{1/2}$, even though the correlation was no longer dimensionless. The separation between the 2.5 cm and 10 cm (1" to 3.9") pipes is also in evidence for the University of Alberta data, as shown in Fig. 6. The data indicates that there may be lower limit of pipe size for scalability of at least 7.5 cm (3") in the wake-stabilized regime, even though the flow conditions are very different from the jetting regime.

3.8 Scale-up and Dimensionless Parameters

We have shown the dimensionless parameters that have been used to attempt to correlate the performance of flares over limited data sets. We have also identified the different regimes in which there is limiting behavior for the independent variables. There is also evidence for a minimum pipe size of at least 7.5 cm (3") for scale-up for both the jetting and wake-stabilized regimes.

In the EER tests (Pohl and Solberg, [1984, 1985, 1986]) conducted in the buoyant and jetting regimes, the results were compared to the operating range of full-scale refinery flares in a plot of pipe Reynolds number and Richardson number. These are

$$\mathrm{Re}_p = \frac{D_p U_f}{\nu_f} \quad \text{and} \quad Ri = \frac{g D_p}{U_f^2} \tag{3-31}$$

Each of these have both the flare gas exit velocity and diameter. They can be re-arranged to give dimensionless velocity and diameter

$$V_f^* = \left(\frac{\mathrm{Re}_p}{Ri}\right)^{1/3} = \frac{U_f}{(\nu_f g)^{1/3}} \quad \text{and} \quad D^* = \left(\mathrm{Re}_p^2\, Ri\right)^{1/3} = D_p\left(\frac{g}{\nu_f^2}\right)^{1/3} \tag{3-32}$$

If the Reynolds number and Richardson numbers are sufficient to relate the behaviors in the jetting regime, then equation (3-32) shows that changing the viscosity of the flare gas can relate different exit velocities and different pipe diameters.

3.8.1 EXPLAINING THE '3 INCH RULE' IN THE JETTING REGIME

It was noted earlier that there appears to be a minimum pipe size of 3 inches (7.5 cm) for the flare combustion efficiency to scale-up to larger sizes. We are calling this the "3 inch rule". The simplest explanation of this minimum pipe size in the jetting regime is geometrical. Near the exit of the flare pipe, the mixing of the air with the flare gas is proportional to the perimeter of the jet while the mass of flare gas to be mixed is proportional to the area. The ratio of perimeter to area varies as the reciprocal of the pipe diameter, so that it is large for small pipes and goes to zero for large pipes. For example, a 1" flare has a perimeter to area ratio of 4, while a 20" flare has a ratio of 0.2. This order of magnitude difference limits the ability to scale results. Modern advanced industrial flares have a ratio around 0.6 (Baukal and Schwartz, 2000).

A more complicated explanation considers the viscous boundary layer thickness for fully developed turbulent pipe flow with superficial velocity U_f. As the flow exits the pipe, the boundary layer is important for the initial mixing of air and fuel, affecting the stability of the flame. The thickness of the boundary layer δ next to the pipe wall (viscous wall region) changes with the Reynolds number for the flow in the pipe Re_p. The ratio of the viscous boundary layer thickness to the pipe diameter $\Delta = \delta / D_p$ is given by the equation (Pope 2000).

$$\Delta = 27.4\,\mathrm{Re}_p^{-0.88} \tag{3-33}$$

The experiments to determine the maximum exit velocity used a fixed pipe size and fuel composition; the exit velocity is increased until blow-off occurs. This means the pipe Reynolds number is increased and the ratio of viscous boundary layer thickness to pipe diameter is decreased. In Fig. 17 we have plotted the ratio against the pipe diameter for flare gas exit velocity from 50 m/s to 200 m/s (164 ft/s to 656 ft/s), the range of observed maximum exit velocities.

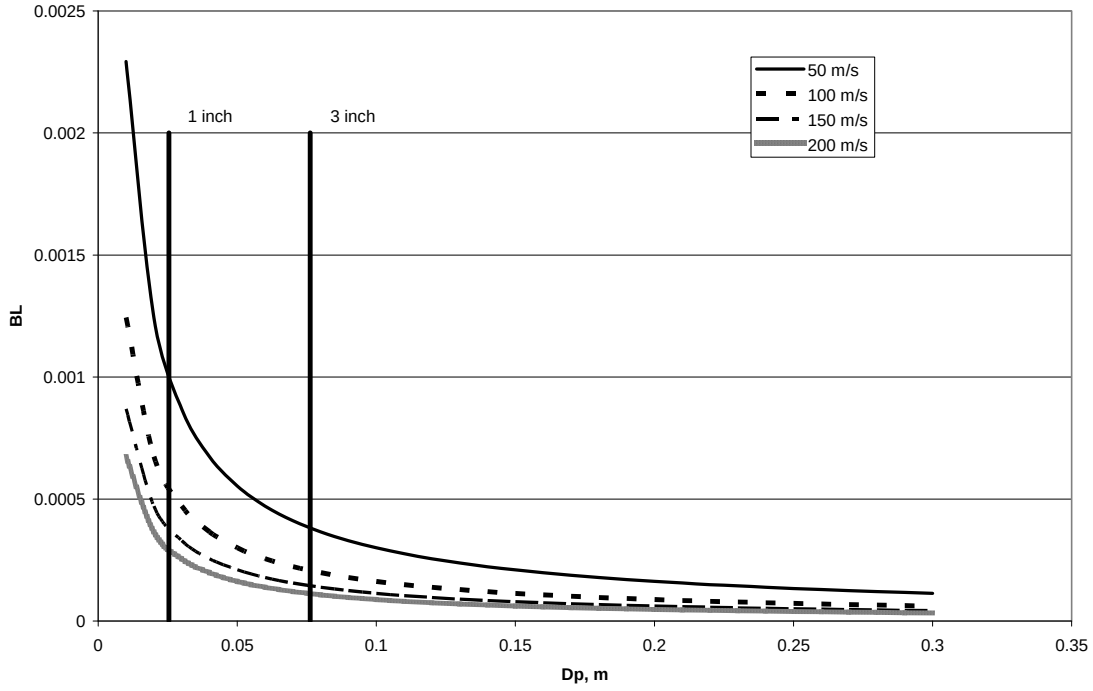

Figure 17 - Plot of the ratio of viscous boundary layer thickness to pipe diameter (BL) against pipe diameter for flare gas exit velocities in the observed range of maximum stable velocity.

Vertical lines are placed for 2.5 cm and 7.5 cm (1" and 3") pipes. The wide spread at 2.5 cm (1") indicates the sensitivity of relative size of the boundary layer thickness at the smaller pipe sizes. This means that for these smaller diameter pipes the blow-off experiments are strongly affected by the changing size of the boundary layer thickness as well as the changing combustion conditions. This argument applies to simple pipe flares, which are the design used for this type of experiment and from which the "3 inch rule" has been observed. It does not apply to large, sophisticated industrial flare tips.

3.8.2 EXPLAINING THE '3 INCH RULE' IN THE WAKE-STABILIZED REGIME

We have looked at the various regimes for the wake of a cylinder in a cross-wind as indicated by the Strouhal number, the static drag and dynamic force coefficients in the discussion of the wake-stabilized regime. The plot of cross-wind Reynolds number against wind speed for different pipe diameters is given in Fig. 18. The pipe size ranges from 2.5 cm to 1 m (1" and 39"), which is from lab-scale to full-scale. If there is a significant difference in the wake structure between 2.5 cm and 7.5 cm (1" and 3"), it

should be indicated in this plot. Nothing is evident there. However, it is worth noting that the full-scale flare pipes are almost always in the critical and supercritical regimes, which means a fully turbulent boundary layer thickness on the pipe surface, a smaller turbulent wake, a lower Strouhal number and a lower dynamic force. If these properties of the wake and boundary layer thickness are significant for flare performance in the wake-stabilized regime then the small-scale pipe experiments may not capture the behavior of full-scale flares.

We do not yet have an explanation for the apparent minimum pipe size for the scalable performance in the wake stabilized regime.

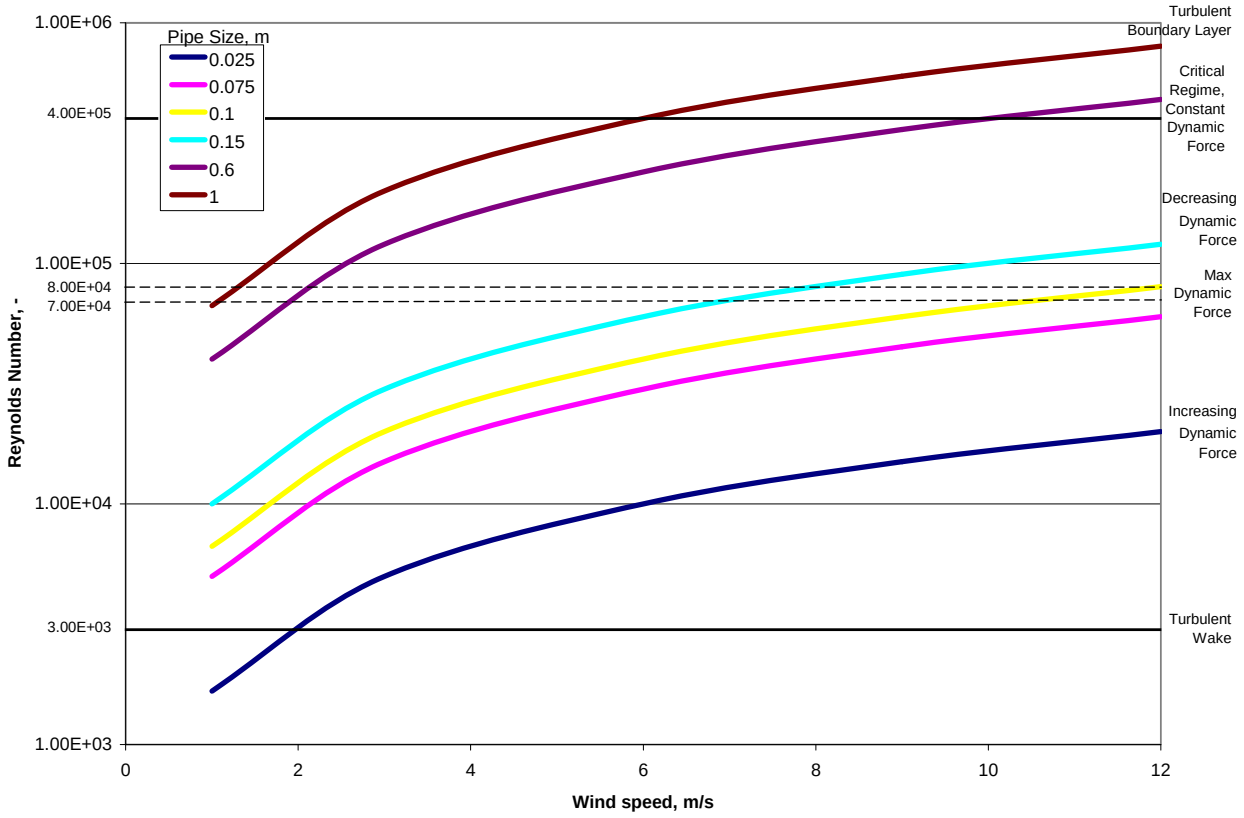

Figure 18 - Wind Reynolds number for pipe sizes from pilot-scale to full-scale. The various regimes for the wake of a long cylinder are indicated.

3.8.3 DIMENSIONLESS PARAMETERS

The dimensionless parameters for the jetting regime are made up of the relevant fuel properties and a suitable dimensionless velocity, such as the Mach number or V_f^* defined in equation (3-32).

The wake stabilized regime has two dimensionless groups under consideration. The Buoyant Plume group is the cube root of the product of the wind Richardson number and the ratio of wind speed and flare gas exit velocity.

$$BP = \frac{U_w}{\left(gD_p U_f\right)^{1/3}} = \left(\frac{U_w^2}{gD}\frac{U_w}{U_f}\right)^{1/3} \tag{3-34}$$

The Power Factor is the cube root of the ratio of the wind power to the power of combustion, and it is composed of the following factors.

$$PF = \left(\frac{\rho_a U_w^3 D_p^2}{\dot{m}_f LHV_m}\right)^{1/3} \propto \left(\frac{\rho_a}{\rho_f}\frac{U_w^2}{LHV_m}\frac{U_w}{U_f}\right)^{1/3} \tag{3-35}$$

Neither dimensionless grouping accounts for the reaction rate or reaction time scale. The obvious choice is to use the laminar flame speed, either the maximum flame speed for the given fuel/air combination or the flame speed for a stoichiometric fuel/air mixture. Also missing is some account of the range of flammable mixtures. This can be provided by the upper and lower air-to-fuel ratios (derivable from the flammability limits) and the stoichiometric air-to-fuel ratio. This gives a long list of dimensionless factors to consider in correlating performance data in the wake stabilized regime,

$$\left\{\frac{\rho_a}{\rho_f}, \frac{U_w^2}{LHV_m}, \frac{U_w}{U_f}, \frac{U_w^2}{gD_p}, \frac{S}{U_w}, AFR_U, AFR_L, AFR_{st}\right\} \tag{3-36}$$

Not all these factors will have independent significance, they may combine to form dimensionless parameters that may describe the behavior, such as the buoyant plume group and power factor. If the observed ratio $\frac{U_w}{U_f^{1/3}}$ (found in the Buoyant Plume group

and Power Factor) continues to be supported by future testing, the only new dimensionless group that can be formed from the list (3-36) is $\frac{U_w}{U_f}\left(\frac{U_w}{S}\right)^2$.

3.9 Conclusion on Major Variables

It was necessary to distinguish between the two limiting regimes for elevated flares: jetting and wake-stabilized. Some guidance was found in the literature on stack design and downwash regarding the main fluid mechanical properties.

There is strong evidence that there is a minimum flare pipe size for proper scaling. That minimum size is at least 7.5 cm ('the 3 inch rule') and it appears to apply to both regimes despite very different flow patterns. The explanation for this minimum size is not clear, though a couple of explanations were advanced for the jetting regime. It is also appears that flare performance is independent of pipe size when the pipe is greater than 7.5 cm in diameter, although the data are only up to 30 cm (12") in the jetting regime, and 15 cm (6") in the wake-stabilized regime.

The flare performance in the jetting regime is dependent only on the exit velocity and the combustion properties of the flare gas. The heat content on a volume basis has been shown to be inadequate, failing to capture the difference between nitrogen and carbon dioxide as inert species, or the stabilizing effect of relatively low amounts of hydrogen. Two correlations for maximum exit velocity have been advanced (Noble et al. [1984] equation 3-25 and Shore [2007] equation 3-26). Both are very sensitive to uncertainty of the flammability limits.

Flare performance in the wake-stabilized regime is dominated by the wind speed. The ratio $U_w / U_f^{1/3}$ seems to indicate the relative contributions of the wind speed and fuel exit velocity in this regime. This is the only clear conclusion for the wake-stabilized regime. The heat content on a mass basis has been used in correlations for combustion inefficiency, but does not fully correlate fuel properties.

The literature does not have data for flare performance during the transition between the regimes, either by changing the exit velocity of the flare gas or by changing the wind speed.

4.0 TRACE EMISSIONS

Trace emissions refer to the chemical species formed during combustion and released into the atmosphere, but are not the products of complete combustion (CO_2, H_2O). The major trace compound is carbon monoxide (CO), which results from interrupted oxidation. There is also soot, a condensed phase composed of carbon, and with the possibility of polyaromatic hydrocarbons (PAHs) or other heavy species in the matrix. There is the possibility of emission of a wide range of intermediate species that are formed during the combustion process. A study of emissions from process heaters (Seebold [1997]) showed that combustion of reagent grade methane can produce measureable quantities of these intermediate species under the extremes of lean and rich firing conditions. Of course, 'measureable' did require some sensitive (in the ppt range) measurement equipment. Elevated flares are diffusion flames but are not controlled as in a furnace and have both lean and rich conditions although they operate in very different temperature regimes.

The other trace emission considered here is the emission of NO_x (NO or NO_2). These species can be form by three possible mechanisms in a combustion system: thermal; prompt; and fuel-nitrogen. Thermal NO_x is the fixing of atmospheric nitrogen at high temperature through the Zeldovich mechanism. Prompt NO_x similarly fixes atmospheric nitrogen but through the attack of hydrocarbon radicals. The intermediates are oxidized to NO. When the fuel has nitrogenous species, these will oxidize partially to NO_x. In the absence of fuel-bound nitrogen, the thermal mechanism is dominant. Nitrous oxide, N_2O, can also be formed in some low temperature combustion systems such as fluidized beds. It is a very strong greenhouse gas with global warming potential about 300 times that of carbon dioxide (I.P.C.C., 2007). It should not be confused with the NO_x species. The formation mechanism for nitrous oxide in combustion requires fuel-bound nitrogen and a suitable temperature window. Nitrogen fertilizers in agricultural use are a much bigger source of nitrous oxide than combustion systems (U.S. E.P.A., 2009).

Emission factors are the method to report trace emissions so that they can be compared. Concentrations cannot be used as they will vary due to varying dilution rates. The emissions factors relate the emissions to the mass rate or the energy rate of the flare gas.

$$\varepsilon_X = \frac{\text{grams of X}}{\text{kg of flare gas}}, \quad \mathrm{E}_X = \frac{\text{grams of X}}{\text{MJ of flare gas}} \tag{4-1}$$

For a species that is in the flare gas, it is impossible to distinguish molecules that pass unreacted from those formed. The emission factor comes directly from the Destruction Efficiency.

$$\varepsilon_X = \frac{100 - DE_X}{100} w_X \tag{4-2}$$

This equation has units mass of X emitted to mass of X in the flare gas.

4.1 Hydrocarbon Emissions

This section's purpose is to compare trace emissions measured by several testing programs. The testing of covered pipe flares with liquid entrainment is also noted.

The emissions of hydrocarbons from a pipe flare were measured as part of the EER work (Pohl and Soelberg [1985]). The special samples were taken with a five-point rake probe in the plume above the flare flame for analysis for hydrocarbons in a GC. As such it is difficult to establish an emission factor. In addition, the use of SO_2 as a tracer seemed to result in the formation of thiophene, or perhaps contamination.

The emissions of trace compounds from associated gas flares were a significant part of the work of Strosher [1996]. The flares were operating in the wake-stabilized regime and there was significant entrainment of liquids into the flare. Although numerous heavy hydrocarbons were detected, this was because the sampling location was in the combustion zone.

The work firing natural gas at the University of Alberta (Kostiuk et al. [2004]) took grab samples in their recirculating wind tunnel which were analysed for PAHs, selected aldehydes (including formaldehye and acetaldehyde), and BTEX. Even though the recirculation of the wind tunnel gases could raise questions because the emissions passed the reaction zone several times, the volume of the reaction zone was very small compared to the total gas volume. In all cases no species were found above the detection limit. For PAHs, this translates into mass emission factors less that 0.01 mg PAH/kg fired. The

other species had a higher detection limit, by about a factor of 40, so the mass emission factors were less than 0.25 mg/kg fired.

The emitted soot from a 2.5 cm (1") pipe firing propane was analysed for PAHs. Detectable amounts of napthalene, acenaphthylene, fluorene, phenanthrene, fluoranthene and pyrene were found. These are predominantly non-carginogenic species. The emission factor for total PAHs was approximately 0.001 g PAH/g soot. The propane flare had conversion of fuel carbon to soot of 0.004 mass soot/mass propane. So the total emission factor of PAHs in the soot was estimated to be 0.004 mg/kg propane fired. Measurements were not taken in the gas phase.

Similar measurements were taken in the single-pass CanmetENERGY Flare Test Facility. To mimic the effect of entrained liquids in the Strosher [1996] work, a pressure-atomization nozzle was used to introduce small liquid droplets of commercial gasoline into the flare gas. Canister samples were taken simultaneously at the air inlet and in the stack and analysed for VOCs. Also, particulate samples were taken and analyzed for PAHs. The mass of particulate gathered was less than 1 mg/m^3.

The VOC species detected above the levels in the ambient air are shown in Fig. 19.

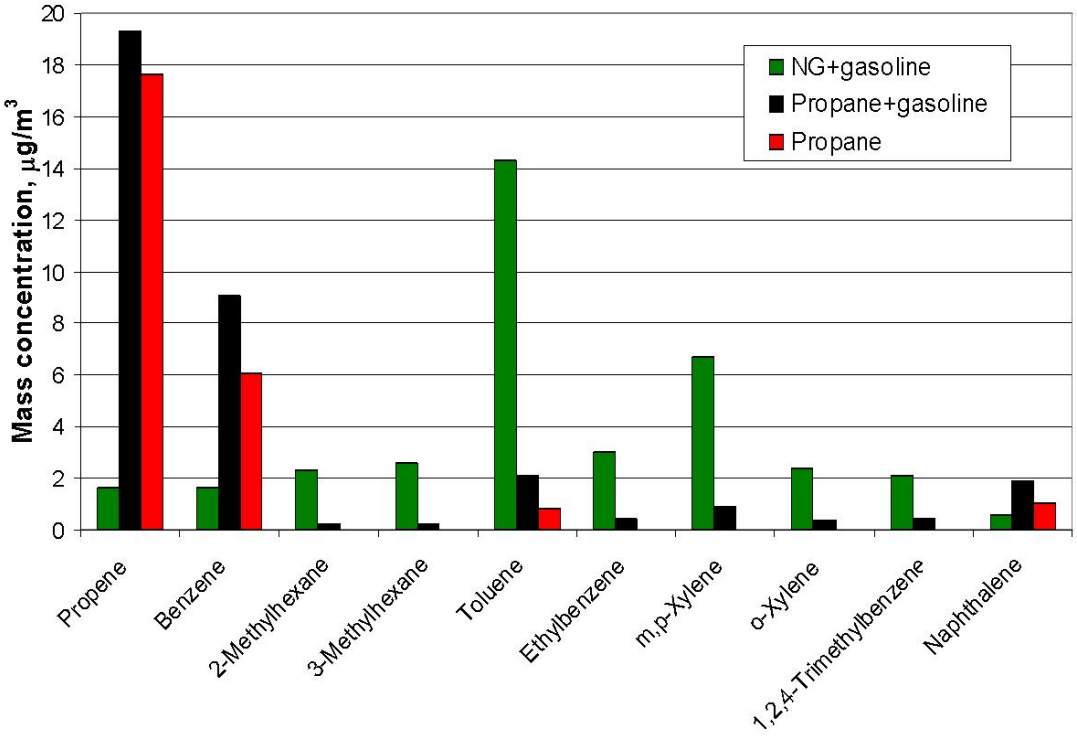

Figure 19 - Measured VOC emissions at the CanmetENERGY FTF as the mass of VOC in volume of stack gas. The compounds emitted from natural gas with gasoline can be attributed to unburned components in the gasoline.

None were found for natural gas by itself. For propane alone, the species found were propene (propylene), benzene, toluene and naphthalene. For natural gas and propane with gasoline addition, the species found can be attributed to the unburned components of the gasoline.

The analysis of PAH species in the soot found in the CanmetENERGY FTF and found in the CMA tests (McDaniel 1983) are shown in Fig. 20. The definitions of the abbreviations of the PAH species can be found in Table 7.

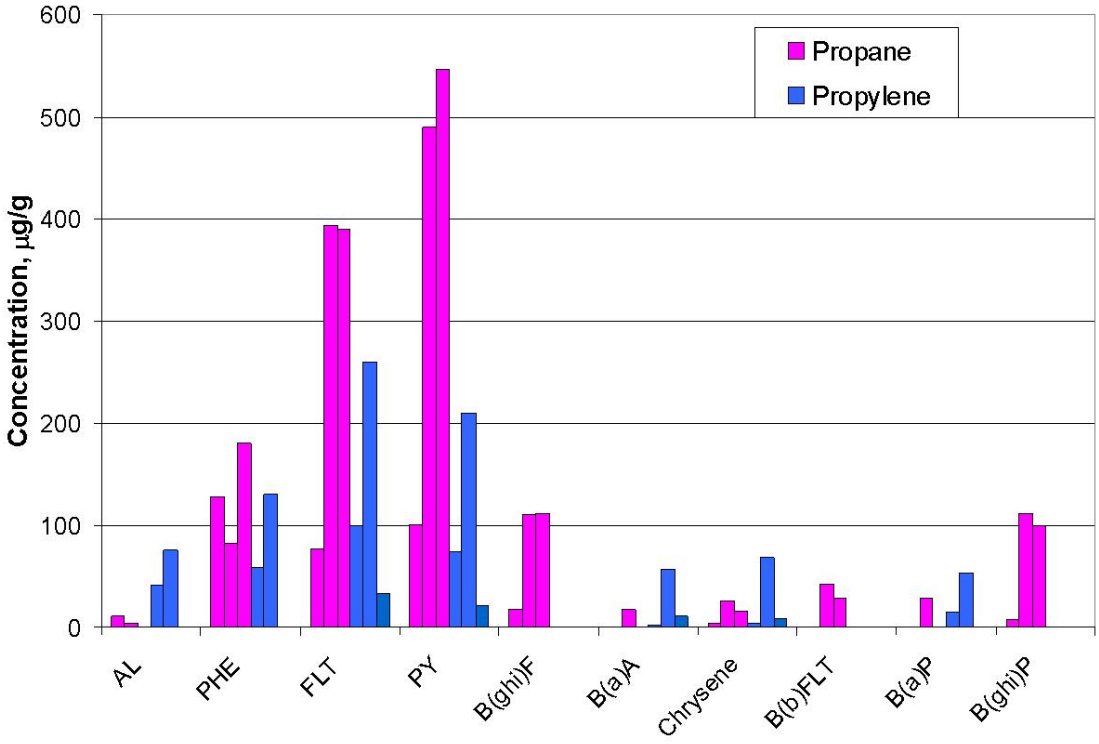

Figure 20 - Concentration of PAH species in the soot emitted from flares from the CanmetENERGY FTF firing propane and the CMA tests firing raw propylene (McDaniel [1983]). The abbreviations are given in Table 7.

Table 7 - List of abbreviations of PAHs used in Fig. 20.

Compound Name	Abbreviation
Acenaphthylene	AL
Fluorene	FL
Phenanthrene	PHE
Anthracene	AN
Fluoranthene	FLT
Pyrene	PY
Benzo(ghi)fluoranthene	B(ghi)F
Benz(a)anthracene	B(a)A
Chrysene	Chrysene

The main species are acenaphthylene, phenanthrene, fluoranthene and pyrene for both sets of measurements. These are the same species found by the University of Alberta. It seems that the composition of PAHs in the soot is independent of the fuel fired.

Both sets of controlled experiments in the wake-stabilized regime, at CanmetENERGY and at University of Alberta, failed to find the level of emissions reported by Strosher [1996]. The results from CanmetENERGY indicate that entrained liquid will not combust completely and the emissions found by Strosher are likely uncombusted compounds found in the entrained liquids.

4.2 NO_x Emissions

The emission factor, E_X, for NO_x was reported in Pohl and Soelberg [1985] as lb NO_2/MMBtu fired. The emission factor was correlated with the heat release rate $\dot{Q}$ (MMBtu/h) as

$$E_X \approx 10^{-3}\dot{Q} \tag{4-3}$$

This emission factor is for fuels containing hydrocarbons only; the emission factor for fuel-bound nitrogen species was higher by two orders of magnitude and depended on the concentration of nitrogenous species in the flare gas.

5.0 CONCLUSIONS

We have surveyed the literature on the performance and emissions for elevated flares. The major independent variables that affect flare performance and flare efficiency are: wind speed, flare gas exit velocity, flare gas composition, flare pipe diameter, and steam assist rate. We have also distinguished two limiting regimes, determined by the relative strength of the flare gas jet and the wind speed. The momentum flux ratio has been suggested as the likely parameter for identifying the boundaries for the regimes. The jetting regime has a strong flare gas jet, strong enough to dominate wind effects, at least near the exit from the flare pipe. The wake-stabilized regime has a weak flare gas jet and strong wind, so that the flare flame is stabilized in the wake of the flare tip. This regime is dominated by the cross-wind and the properties of the wake. Flaring studies have predominantly evaluated model flares in either of these two regimes. Therefore, it is important to limit the conclusions drawn from the studies to simple pipe flares operating within the regime in question.

The jetting regime has been the most extensively studied. It has been shown that a jetting flare will have destruction efficiency above 98% as long as the exit velocity is less than the maximum exit velocity for the given flare gas composition. Destruction efficiency decreases discontinuously as the maximum exit velocity is approached. It has been shown that the heat content on a volume basis is not an adequate measure for the flare gas composition. It does not account for the stabilizing effect of hydrogen, nor does it account for the differing effects of inert compounds, particularly nitrogen and carbon dioxide. The "stability curve" for exit velocity has been shown to be independent of pipe size for diameters of 7.5 cm (3 inches) and larger. While the "3 inch rule" gives confidence about the applicability of pilot-scale testing to full-scale flares, it does mean the research using smaller diameter pipes in the jetting regime has questionable value for full-scale flares.

The wake-stabilized regime has been studied mostly in the context of production flares – small, low flow, continuous operation – with a relatively narrow range of gas composition. Unlike the jetting regime, flare efficiency changes continuously with wind speed and flare gas exit velocity. The ratio $U_w / V_f^{1/3}$ correlates this change of flare

efficiency. There are recirculating eddies attached in the wake of the pipe. Inefficiency in the wake stabilized regime comes from the stripping of fuel from these eddies by the flow generated in the wake of the flare tip. Despite having a completely different fluid flow pattern, the wake-stabilized regime seems to also have a minimum pipe size of 7.5 cm for scaling the results. We have not found a fully acceptable explanation for why the "3-inch rule" apparently applies to wake-stabilized flares.

The following are eight areas of the flare performance that need to be addressed:

1. Experimental studies of the flare efficiency in the transition between jetting and wake-stabilized regimes.
2. Experimental studies of the effect of wind on steam-assisted flares.
3. Experimental studies on the limiting hydrogen concentration for steam-assisted flares, and wind blown flares.
4. HRVOC and NO_x measurements for flares with and without steam-assist.
5. Develop the combination of fuel properties to correlate the flare efficiency with flare gas composition, particularly accounting for the special case of hydrogen, and the inert gases nitrogen and carbon dioxide.
6. Develop a treatment of steam-assist rate that includes the flare gas composition, perhaps unifying steam with the handling of nitrogen and carbon dioxide dilution.
7. Need to expand areas of flare performance to include higher capacity flare burners with specific design features that are commonly used in refinery and chemical plants.
8. Need to address environmental regulators' requirements by testing flares similar to those used by industry.

Additional flare testing on a full-scale flare burner with steam-assist is also recommended to address the following five issues:

1. Direct measurement of flare emissions using remote measurements.
2. Large diameter flare testing such as >30 inch (76 cm) of steam assist configuration.

3. Tests conducted at maximum and minimum (< 1%) flare flow rates.
4. Full-scale flare testing at multiple wind speeds.
5. Full-scale flare testing with up to 80%-v inert gases.

6.0 REFERENCES

Baukal, C.E. and Schwartz, R.E. [2000] "The John Zink combustion handbook", CRC Press.

Becker, R. [1974] "Ausbrandmessungen an Fackelflamen" (Measurement of residuals of flare stacks – in German), Messen + Steuern, **32**, pp. 23-25.

Blackwood, Thomas R. [2000] "An Evaluation of Flare Combustion Efficiency Using Open-Path Fourier Transform Infrared Technology." Journal of the Air & Waste Management Association, **50,** pp. 1714-1722.

Boden, J.C., Tjessem, K.l., Wotton, A.G., and Moncrieff, J.T.M. [1996] "Elevated flare emissions measured by remote IFC sensing." Petroleum Review, pp. 524-528.

Bourguignon, E., Johnson, M.R., and Kostiuk, L.W. [1999] "The use of a closed-loop wind tunnel for measuring the combustion efficiency of flames in a cross flow." Combustion and Flame, **119,** pp.319-334.

Coward, H.R. and G.W. Jones [1952] "Limits of flammability of gases and vapours." Bulletin 503, Bureau of Mines.

Dubnowski, John J., and Davis, Bruce C. [1983] "Flaring Combustion Efficiency. A Review of the State of Current Knowledge." APCA, **10**, pp .27.

EER [1997]"Hydrogen Flare Equivalency Demonstration (Final Report)." Report to E.I. du Pont de Nemours and Company.

Fells, I. and Rutherford, A.G. [1969] "Burning Velocity of Methane-Air Flames." Combustion and Flame, **13**, pp. 130-138.

Gogolek, P., Hayden, A.C.S., and Madrali, S. [2001] "Performance and Speciation of Solution Gas Flares Tested in the CANMET Flare Test Facility - Final Report." CETC report to PTAC.

Gogolek, P.E.G., and Hayden, A.C.S. [2004] "Performance of flare flames in a crosswind with nitrogen dilution." Journal of Canadian Petroleum Technology, **43,** pp. 43-47.

Harris, J. and Lovelace, D.E. [1968] "Combustion characteristics of natural gas and manufactured substitutes." J. Inst Gas Eng., **8**, p. 169-195.

Haus, Rainer, Wilkinson, Rob, Heland, Jorg, and Schafer, K. [1998] "Remote sensing of gas emissions on natural gas flares." Pure and Applied Optics, **7**, pp.853-862.

Hirasawa, T., C.J. Sung, A. Joshi, Z. Yang, H. Wang, and C.K. Law [2002] "Determination of laminar flame speeds using digital particle image velocimetry: Binary fuel blends of ethylene, n-butane, and toluene." Proceedings of the Combustion Institute, **29**, pp. 1427-1434.

Howell, L.W., Poudenx, P.D., Johnson, M.R., Wilson, D.J. and Kostiuk, L.W. [2003]. "Flare Stack Diameter Scaling." Combustion Canada Conference 2003, Calgary, AB.

IPCC (International Panel on Climate Change) [2007] Fourth Assessment Report (AR4) by Working Group 1.

Johnson, Matthew R., Majeski, Adrian J., Wilson, David J., and Kostiuk, Larry W. [1998] "The Combustion Efficiency of a Propane Jet Diffusion Flame in Cross Flow." Fall Meeting of the Western States Section of the Combustion Institute, Seattle, Washington, 98F-38.

Johnson, M.R., and Kostiuk, L.W. [1999] "Effects of a Fuel Diluent on the Efficiencies of Jet Diffusion Flames in a Crosswind." The Combustion Institute, Canadian Section, 1999 Spring Technical Meeting, Edmonton, AB.

(a) Johnson, M.R., Zastavniuk, O., Wilson, D.J., and Kostiuk, L.W. [1999] "Efficiency Measurements of Flares in a Cross Flow." Combustion Canada 1999, Calgary, AB.

(b) Johnson, M.R., Zastavniuk, O., Dale, J.D., and Kostiuk, L.W. [1999] "The Combustion Efficiency of Jet Diffusion Flames in Cross-flow." Joint Meeting of the United States Sections - The Combustion Institute.

Johnson, M.R., and Kostiuk, L.W. [2000] "Efficiencies of Low-Momentum Jet Diffusion Flames in Crosswinds." Combustion and Flame, **123**, pp. 189-200.

Johnson, M.R., Wilson, D.J., Kostiuk, L.W. [2000] "A Fuel Stripping Mechanism for Low-momentum Jet Diffusion Flames in a Crossflow."Combustion Science and Technology, **169**, pp. 155-174.

Johnston, C.R., and Wilson, D.J. [1997] "A Vortex Pair Model for Plume Downwash into Stack Wakes." Atmospheric Environment, **31**, pp. 13-20.

Joseph, D., Lee, J., McKinnion, C., Payne, R., and Pohl, J. [1983] "Evaluation of the Efficiency of Industrial Flares: Background-Experimental Design-Facility." EPA Report No. 600/2-83-070.

(a) Kalghatgi, G.T. [1981] "Blow-Out Stability of Gaseous Jet Diffusion Flames. Part I: In Still Air", Combustion Science and Technology, **26**, pp. 233-239.

(b) Kalghatgi, G.T. [1981] "Blow-Out Stability of Gaseous Jet Diffusion Flames. Part II: Effect of Cross Wind", Combustion Science and Technology, **26**, pp. 241-244.

Karim, G.A., Wierzba, I. and Boon, S. [2004] "Some considerations of the lean flammability limits of mixtures involving hydrogen." International Journal of Hydrogen Energy, **10**, pp. 117-123.

Keller, Mike, and Noble, Roger [1983] "RACT for VOC - A Burning Issue." Pollution Engineering Magazine.

a) Kostiuk, L.W., Johnson, M.R., and Prybysh, R.A. [2000] "Recent Research on the Emission from Continuous Flares." Combustion and Environment Group, Department of Mechanical Engineering, University of Alberta.

b) Kostiuk, L.W., Majeski, A.J., Poudenx, P., Johnson, M.R., Wilson, D.J. [2000] "Scaling of Wake-Stabilized Jet Diffusion Flames in a Transverse Air Stream", Proceedings of the Combustion Institute, **28**, pp. 553-559.

Kostiuk, L.W., Johnson, M.R., and Thomas, G. [2004] "University of Alberta Flare Research Project Final Report November 1996 – September 2004" Combustion and Environment Group, Department of Mechanical Engineering, University of Alberta.

Leahey, D.M, and Schroeder, M.B. [1987] "Observations and predictions of jet diffusion flame behaviour." Atmospheric Environment, **21**, pp. 777-784.

Leahey, D.M., Preston, K., and Strosher, M. [2001] "Theoretical and Observational Assessments of Flare Efficiencies." J. Air & Waste Management Assoc. **51** pp. 1610-1616.

Lee, Kun-Chieh, and Whipple, Gary M. [1981] "Waste Gaseous Hydrocarbon Combustion in a Flare." 74th APCA Meeting.

Lyons, K.M. [2007] "Toward an understanding of the stabilization mechanisms of lifted turbulent jet flames: experiments", Progress in Energy and Combustion Science, v.33, pp.211–31.

McDaniel, M. [1983] "Flare Efficiency Study." EPA-600/2-83-052.

Mellqvist, J. [2001] "Flare testing using the SOF method at Borealis Polyethylene in the summer of 2000." Chalmers University of Technology.

Molnarne, M., P. Mizsey, and V. Schroder [2005] "Flammability of gas mixtures Part 2: Influence of inert gases." Journal of Hazardous Materials, **A121**, pp. 45-49.

Noble, R.K., Keller, M.R. and Schwartz, R.E., [1984] "An Experimental Analysis of Flame Stability of Open Air Diffusion Flames." American Flame Research Committee International Symposium on Alternate Fuels and Hazardous Wastes, Tulsa, OK.

Overcamp, T.J. [2001] "A review of the conditions leading to downwash in physical modeling experiments." Atmospheric Environment, **35**, pp. 3503-3508.

Ozumba C.I., and Okoro, I.C. [2000] "Combustion Efficiency Measurements of Flares Operated by an Operating Company." SPE International Conference on Health, Safety and the Environment in Oil and Gas Exploration and Production pp. 1-11.

Payman, W. and Wheeler, R.V. [1922] "The Composition of Gaseous Fuels in Relation to their Utilisation." Fuel Sci Pract, **1**, pp. 185.

Pohl, J.H., Payne, R., and Lee, J. [1984] "Evaluation of the Efficiency of Industrial Flares: Test Results." EPA-600 /2-84-095.

Pohl, J.H., and Soelberg, N.R. [1985] "Evaluation of the Efficiency of Industrial Flares: Flare Head Design and Gas Composition". EPA-600/2-85-106.

Pohl, J.H., and Soelberg, N.R. [1986] "Evaluation of the Efficiency of Industrial Flares: H_2S Gas Mixtures and Pilot Assisted Flares". EPA-600/2-85-106.

Pohl, J., P. Gogolek, J. Seebold, R. Schwartz [2004] "Fuel Composition Effect on Flare Flame Inefficiency". AFRC/JFRC Joint Meeting, Maui, Hawaii.

Pope, S.B. [2000] "Turbulent Flows", Cambridge University Press, Cambridge, U.K.

Rajaratnam, N. [1976] "Turbulent Jets", Elsevier Scientific Pub. Co., Amsterdam, NL.

Robinson, R.W and J. Hamilton [1992] "A criterion for assessing wind induced crossflow vortex vibrations in wind sensitive structures", Health and Safety Executive – Offshore Technology Report, HMSO, London.

Romano, R.R. [1983] "Control Emissions with Flare Efficiency." Hydrocarbon Processing, **62**, pp. 78-80.

Scholte, T.G. and P.B. Vaags [1959] "Burning Velocities of Mixtures of Hydrogen, Carbon Monoxide and Methane with Air." Combustion and Flame, **3**, pp. 511-524.

Seebold, J.G. [1997] "The Origin and Fate of Toxis Combustion Byproducts in Refinery Heaters: Research to Enable Efficient Compliance with the Clean Air Act", PERF Project 92-19, Final Report August 5, 1997.

Seebold, J.G., Davis, B.C., Gogolek, P.E.G., Kostiuk, L.W., Pohl, J.H., Schwartz, R.E., Soelberg, N.R., Strosher, M., and Walsh, P.M. [2003] "Reaction Efficiency of Industrial Flares: The Perspective of the Past." Combustion Canada '03, Vancouver, BC.

Shore, D [2007] "Improving Flare Design – From Art to Science." AFRC-JFRC 2007 Joint Meeting, Waikoloa, Hawaii.

Siegel, K.D. [1980] “Degree of Conversion of Flare Gas in Refinery Elevated Flares.” Ph.D. Thesis in Engineering Science, University of Karlsruhe, February. (in German and translated into English by The Language Center, Inc.)

Skrbić, B., J. Cvejanov, and M. Peruničić [1985] “Selection of Mixing Rule for the Prediction of the Laminar Burning Velocity for Multicomponent Gas Mixture.” Hungarian Journal of Industrial Chemistry, **13**, pp. 199-206.

Spalding, D.B. [1954] “A Mixing Rule for Laminar Flame Speed.” Fuel, **35**, pp. 347.

Straitz, J.F. [1977], “Make the Flare Protect the Environment.” Hydrocarbon Processing, **56**, pp. 131-135.

Straitz, J.F., [1978] "Flaring for Gaseous Control in the Petroleum Industry." 1978 Annual APCA Meeting, June 29.

Strosher, M. [1996] "Investigations of Flare Gas Emissions in Alberta (Final Report 1996)." Alberta Research Council.

Tatom, F.B. [1986] “Predictions of stack plume downwash.” Journal of Fluids Engineering, **108**, pp 379-382.

URS Corporation. [2004] "Passive FTIR Phase I Testing of Simulated and Controlled Flare Systems: FINAL REPORT”, prepared for the Texas Commission on Environmental Quality, http://www.tceq.state.tx.us/assets/public/implementation/air/am/contracts/reports/oth/Passive_FTIR_PhaseI_Flare_Testing_r.pdf

U.S. E.P.A. [2009] “Climate Change – Nitrous Oxide”, http://www.epa.gov/nitrousoxide/sources.html, retrieved on Dec. 2, 2009.

Yumlu, V.S. [1967] “Prediction of burning velocities of carbon monoxide-hydrogen-air flames.” Combustion and Flame, **11**, pp. 190-194.

Yumlu, V.S. [1968] “The effects of additives on the burning velocities of flames and their possible prediction by a mixing rule.” Combustion and Flame, **12**, pp. 14-18.

Zabetakis, M.G. [1965] “Flammability characteristics of combustible gases and vapours.” Bulletin 627, Bureau of Mines.

.

7.0 APPENDIX

Imperial unit figures and tables:

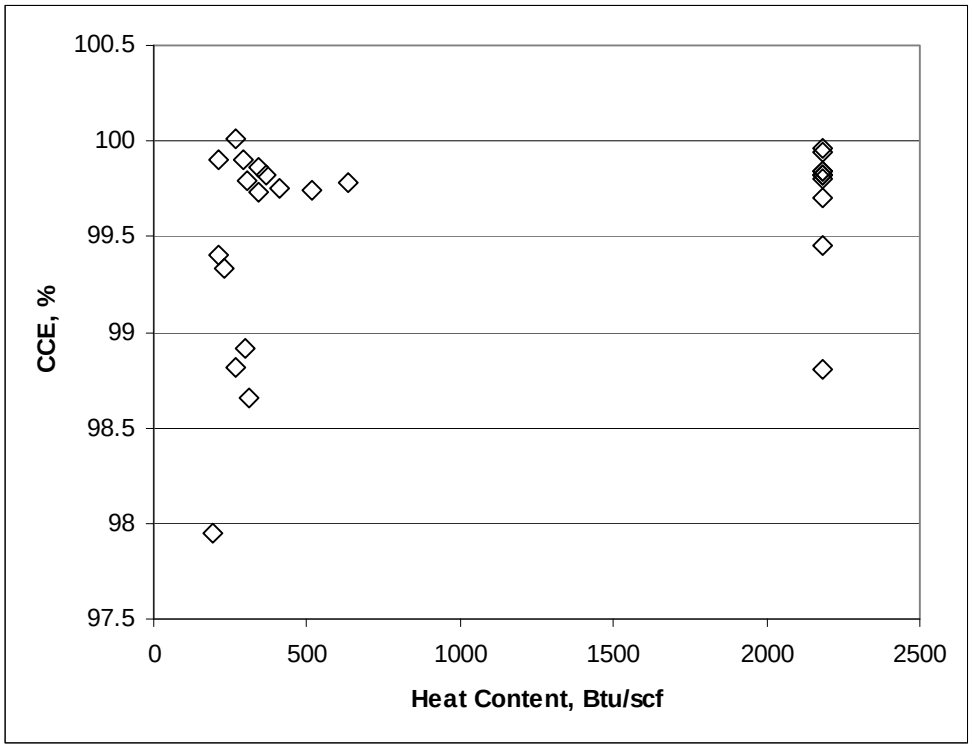

Figure 21 - The effect of nitrogen dilution of propylene on combustion efficiency without steam assist, from the CMA study (McDaniel [1983]).

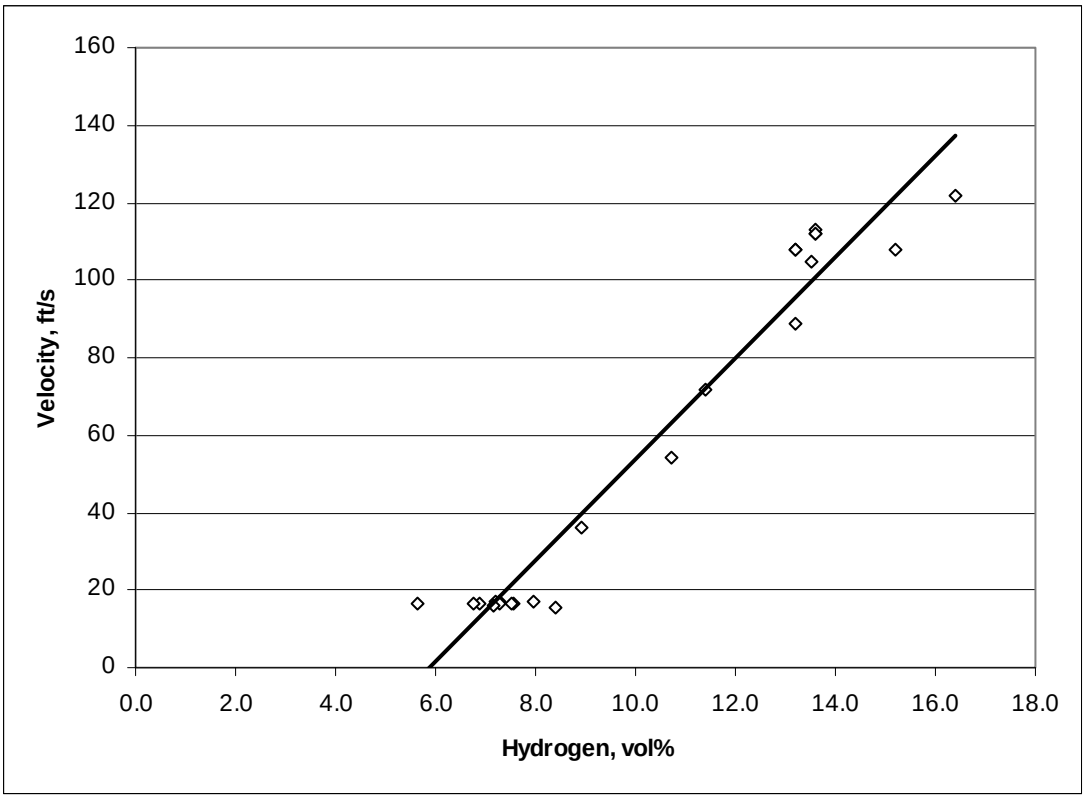

Figure 22 - Lift-off data from EER[1997] without a pilot burner, with the correlation for stability with and without a pilot burner.

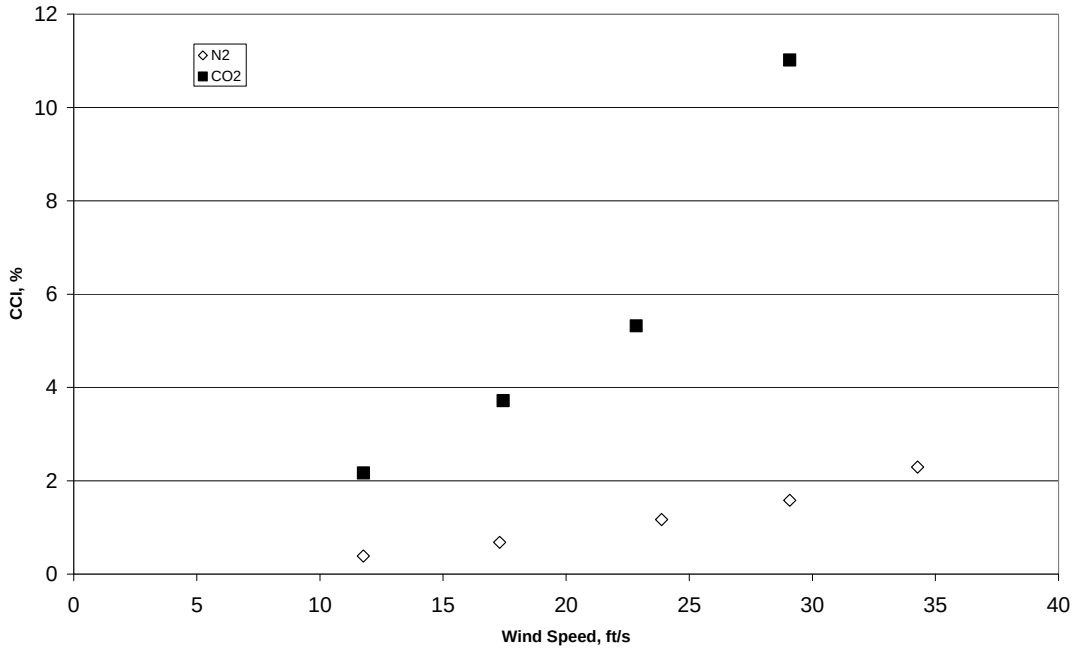

Figure 23 - Combustion Inefficiency for natural gas diluted with 60%-vol nitrogen and carbon dioxide, 4" pipe. The flame blew out at the top wind speed of 27 m/h with carbon dioxide dilution. Data from Gogolek and Hayden [2004].

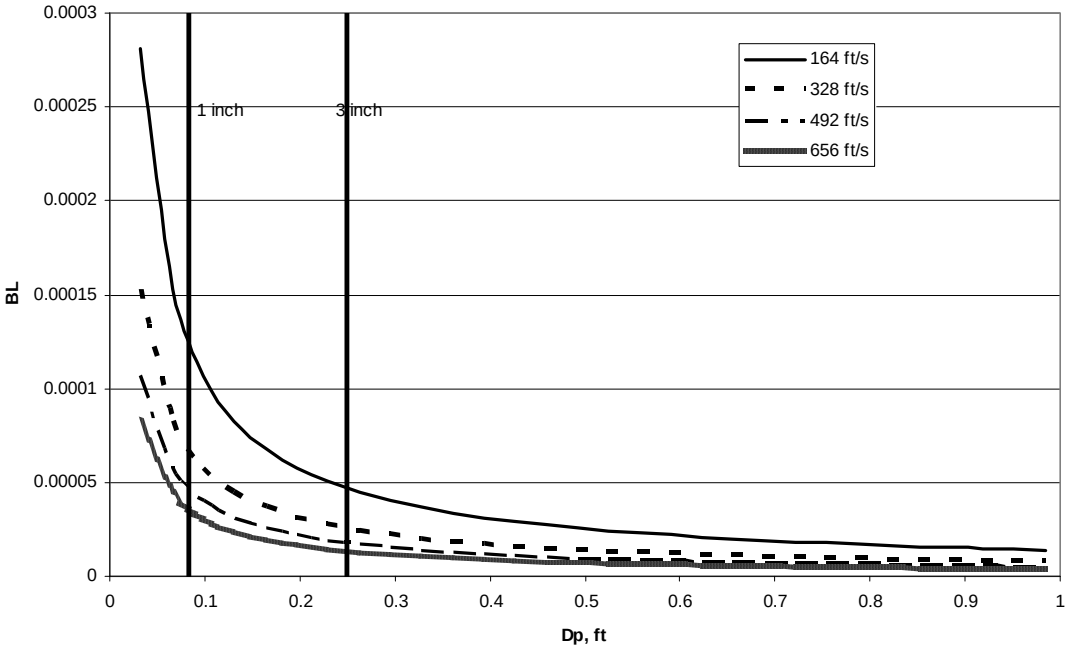

Figure 24 - Plot of the ratio of viscous boundary layer thickness to pipe diameter (BL) against pipe diameter for flare gas exit velocities in the observed range of maximum stable velocity.

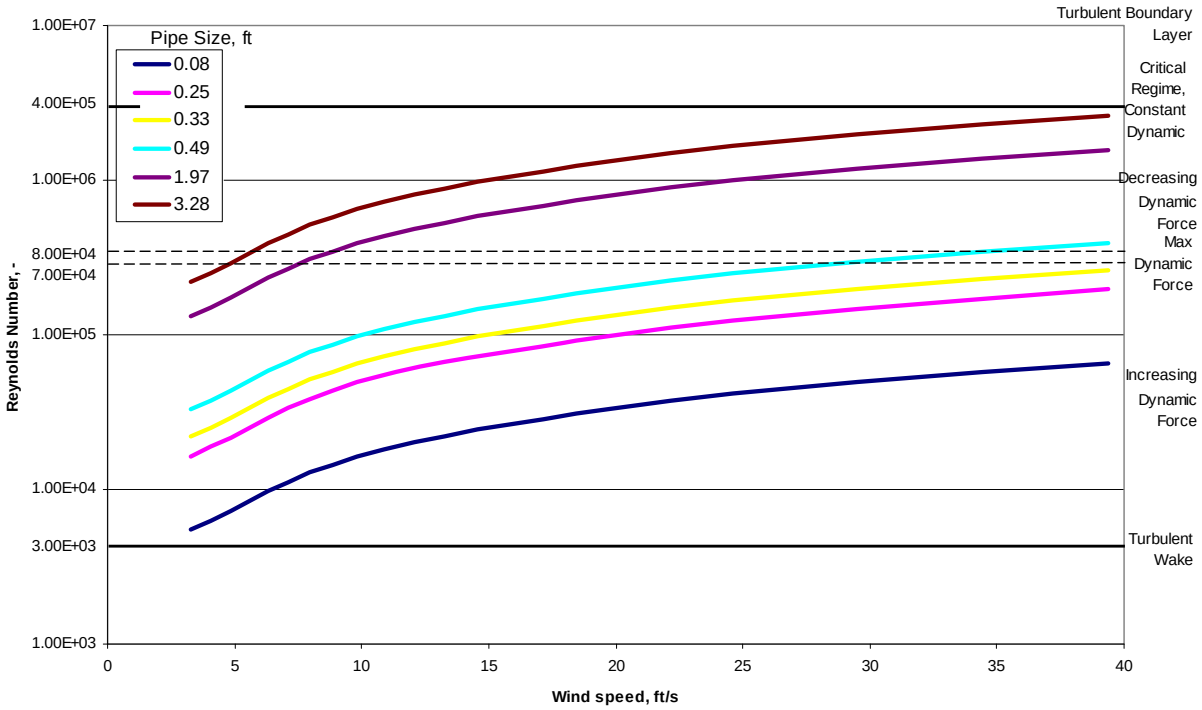

Figure 25 - Wind Reynolds number for pipe sizes from pilot-scale to full-scale. The various regimes for the wake of a long cylinder are indicated.

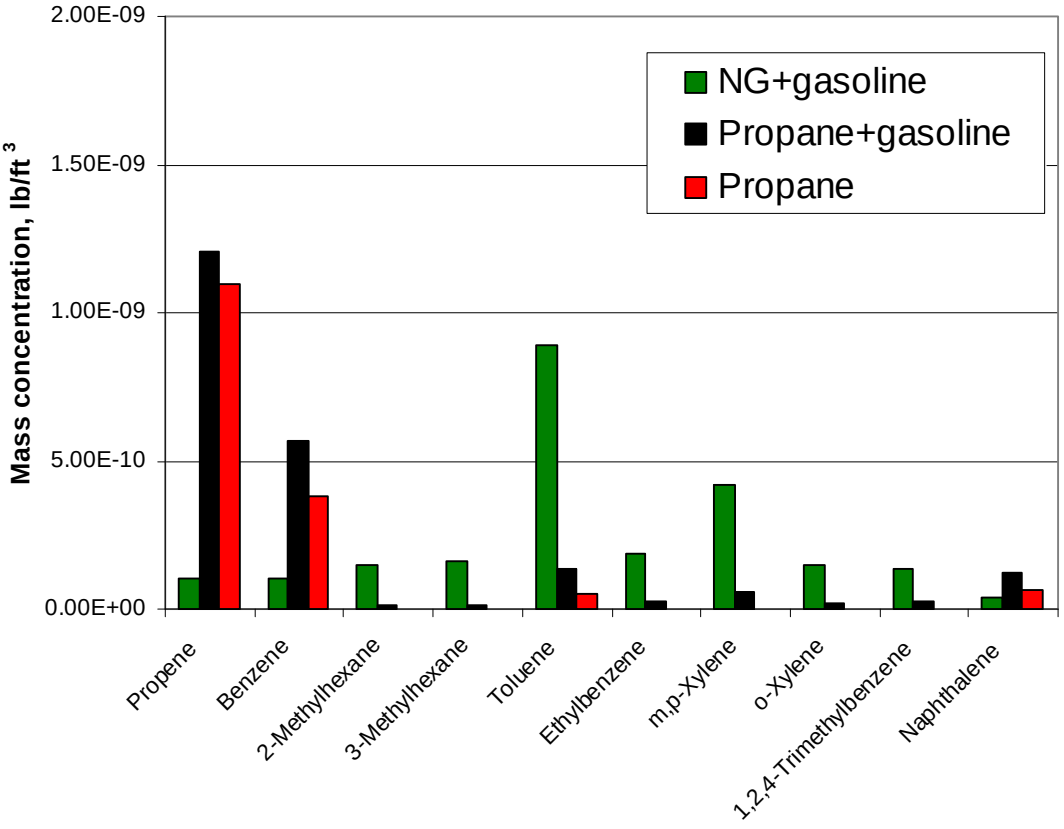

Figure 26 - Measured VOC emissions at the CanmetENERGY FTF as the mass of VOC in volume of stack gas. The compounds emitted from natural gas with gasoline can be attributed to unburned components in the gasoline.

Table 8 - Combustion properties of selected combustible gases.

	Density	**LHV**		**Air:Fuel**		S_{st}	**LFL**	**UFL**	**SFR**
Species	**lb/ft^3**	**Btu/ft^3**	**Btu/lb**	**vol/vol**	**lb/lb**	**ft/s**	**%**	**%**	**lb/lb**
CH_4	0.04	1009	23818	9.55	17.20	1.33	5	15	-
C_2H_6	0.08	1771	22313	16.71	15.90	1.39	3	13	0.1 – 0.15
C_3H_8	0.12	2523	21668	23.87	15.25	1.44	2.1	9.5	0.25 –0.3
C_2H_4	0.07	1602	21625	14.32	14.81	2.16	2.75	34	0.4 – 0.5

C_3H_6	0.11	2338	21023	21.48	14.81	2.30	2	10	0.5 – 0.6
H_2	0.01	325	61049	2.39	34.29	6.89	4	74.2	-
CO	0.07	322	4342	2.39	2.47	0.93	12.5	74.2	-
H_2S	0.17	596	6535	7.16	6.09	1.28	4.3	45.5	-

Summary Table of Flaring Studies Referenced in the Literature Review

Reference	Report Scope	Diameter	Fuels	Assist Media	Wind
Becker [1976]	Limited tests on a small pipe in a wind tunnel.	2.0 cm	Natural gas		Y
Straitz [1977, 1978]	Efficiency of assisted- and unassisted model flares.	5.1, 7.6, 15.2 cm	Natural gas, propane	Steam	
Siegel [1980]	Commercial flare with slip stream of actual refinery relief gas with blower to simulate effect of wind.	20.3 cm	RRG	Steam SFR up to 1.8	Y Up to 6 m/s.
Kalghatgi (a) [1981]	Blow off stability of small pipes	0.1-1.2 cm	CH_4, C_3H_8, C_2H_4, C_2H_2, H_2, C_3H_{10}, CH_4/CO_2, CH_4/air, C_3H_8/CO_2, C_3H_8/air		
Kalghatgi (b) [1981]	Blow off and blow out of small pipes in wind tunnel	0.1-2 cm	CH_4, C_3H_8, C_2H_4, C_2H_2, H_2, C_3H_{10}, CH_4/CO_2, CH_4/air, C_3H_8/CO_2, C_3H_8/air		Y Up to 8 m/s.
Lee and Whipple [1981]	Peculiar flare tip (perforated nozzle with 35% open are)	5.1 cm	C_3H_8		
McDaniel [1983], Keller et al. [1983], Romano [1983]	McDaniel [1983] is the main report, others are summary publications. Testing of assisted and unassisted flares with single point sampling of plume.	20.3 cm	C_3H_6, C_3H_6/N_2	Steam, air	
Noble et al. [1984]	Determining blow-off stability for range of gas mixtures.	7.6 cm	Natural gas, propane, H_2, with N_2 and CO_2		
Pohl et al. [1984]	First report in series, looking at relationship between stability and efficiency for simple pipe flares and 3 commercial designs	Pipe flares – 7.6 cm, 15.2 cm, 30.4 cm; commercial tips – 30.4 cm.	C_3H_8, C_3H_8/N_2		
Pohl and Soelberg [1985]	Second report covering the effect of commercial flare head design and gas composition. Found minimum size below which scale-up is problematic.	Commercial designs: 2 @ 3.8 cm, 9.7 cm, 30.5 cm; gas composition	C_3H_8/N_2 for flare design tests; Propane, ammonia, ethylene oxide, 1-3 butadiene, hydrogen sulphide with nitrogen.	Steam, air	

		testing 7.6 cm.			
Pohl and Soelberg [1986]	Continuing work on flares to include H_2S and pilot burners.	7.6 cm, 15.2 cm	C_3H_8/H_2S, $C_3H_8/H_2S/N_2$		
Boden et al. [1996]	DIAL measurements on emissions from 3 operating flares	2 @ 106 cm, 122 cm	RRG, with H2 from 11%-v to 78%-v.	Steam (ring and center) SFR up to 3	Y Up to 17 m/s.
Strosher [1996]	Point measurements on field flares with entrainment of liquids. Some small lab-scale work.	7.6 cm, 20 cm	Solution gas (sweet and sour) with entrained liquids		Y
EER [1997]	Testing effect of hydrogen content on flare stability	7.4 cm	H_2/N_2 with trace C_2H_4 for HC destruction measurement		
Haus et al. [1998]	Remote passive FTIR measurement of emissions from natural gas production sites	Not reported	Natural gas		Y
Johnson et al. [1998]	First test results from closed-loop wind tunnel flare testing.	2.5 cm	C_3H_8		Y
Bourguignon et al. [1999]	Description of experimental technique for closed-loop wind tunnel testing of small flares.	2.5 cm	Methane		Y
Johnson and Kostiuk [1999]	Effect of dilution on efficiency of small flares in wind tunnel	2.5 cm	CH_4/N_2, CH_4/CO_2, C_3H_8/N_2, C_3H_8/CO_2		Y
Johnson et al. (a) [1999]	Testing of efficiency for exit velocity and wind velocity effects.	2.5 cm	Natural gas, propane		Y
Johnson et al. (b) [1999]	Testing of efficiency for exit velocity and wind velocity.	2.5 cm	Natural gas, propane		Y
Blackwood [2000]	Open path FTIR applied to the plumes from two full-scale stacks	Not reported	CO saturated with water, some trace species.		Y
Johnson and Kostiuk [2000]	Testing of efficiency for exit velocity and wind velocity.	2.5 cm	Natural gas, propane, propane/CO_2		Y
Johnson et al. [2000]	Mapping HC emission near flare flame to identify fuel loss mechanism – stripping.	2.5 cm	Natural gas		Y
Kostiuk et al. (a) [2000]	Interim report on flare studies at University of Alberta	See earlier U Alberta.	See earlier U Alberta.		Y
Kostiuk et al. (b) [2000]	Development of Buoyant Plume parameter to analyze earlier data.	1.1 cm, 1.7 cm, 2.2 cm, 3.3 cm	Propane		Y
Ozumba and Okoro [2000]	Remote measurements on several flares at flow stations.	Not reported	Solution gas		Y

Gogolek et al. [2001]	Report on testing of simple flares in wind tunnel.	2.5 cm, 5.1 cm, 7.6 cm	Natural gas, propane, some with gasoline droplets		Y
Mellqvist [2001]	Use of remote sensing technology (Solar Occultation Flux) to measure DE of ethylene in plume from refinery.	Not reported	RRG, with ethylene content reported.	Steam SFR up to 11.	Y
Howell et al. [2003]	Reporting of larger scale testing of low momentum pipe flares in wind.	2.5 cm, 5.1 cm, 10.2 cm	Natural gas		Y
Gogolek and Hayden [2004]	Effect of nitrogen dilution on flare performance, with and without grid turbulence.	2.5 cm, 5.2 cm, 10.2 cm	Natural gas, natural gas/N_2		Y
Kostiuk et al. [2004]	Final report of University of Alberta work on low momentum flares in wind.	See earlier U Alberta.	See earlier U Alberta.		Y